Article:
Hussein, SO, Lesnic, D and Yamamoto, M (2017) Reconstruction of space-dependent potential and/or damping coefficients in the wave equation. Computers and Mathematics with Applications, 74 (6). pp. 1435-1454. ISSN: 0898-1221

https://doi.org/10.1016/j.camwa.2017.06.030

Reconstruction of space-dependent potential and/or damping coefficients in the wave equation

S.O. Hussein[1], D. Lesnic[2] and M. Yamamoto[3]
[1]*Department Mathematics, University of Sulaimani, P.O. Box 334, Sulaimani, Iraq*
[2]*Department of Applied Mathematics, University of Leeds, Leeds LS2 9JT, UK*
[3]*Department of Mathematical Sciences, The University of Tokyo, 3-8-1 Komaba, Meguro, Tokyo 153, Japan*
E-mails: shilan.husen@univsul.edu.iq, D.Lesnic@leeds.ac.uk, myama@ms.u-tokyo.ac.jp

Abstract
In this paper, nonlinear reconstructions of the space-dependent potential and/or damping coefficients in the wave equation from Cauchy data boundary measurements of the deflection and the flux tension are investigated. This is a very interesting and challenging nonlinear inverse coefficient problem with important applications in wave propagation phenomena. The uniqueness and stability results that are revised and in some cases proved demonstrate an advancement in understanding the stability of the inverse coefficient problems. However, in practice, the inverse coefficient identification problems under investigation are still ill-posed since small random errors in the input data cause large errors in the output solution. In order to stabilise the solution we employ the nonlinear Tikhonov regularization method. Numerical reconstructions performed for the first time are presented and discussed to illustrate the accuracy and stability of the numerical solutions under finite difference mesh refinement and noise in the measured data.

Keywords: Inverse problem; Coefficient identification problem; Carleman estimates; Wave equation; Nonlinear optimization.

1 Introduction

Many practical applications related to wind, wave, seismic or noise excitations require reconstructing the applied loadings/forces/sources from the knowledge of output responses. For example, in Huang (2001), time-dependent external forces in a nonlinear damped vibration system were retrieved from the knowledge of the displacement and velocity at different times. Another application of interest concerns distinguishing between various types of seismic events, e.g., explosion, implosion or earthquake, which generate waves that propagate through the ground and can be recorded using seismometers. In Sjogreen and Petersson (2014), a seismic source modelled as a point moment tensor in the elastic wave equation was estimated from time-dependent wave form measurements. A final related application that is mentioned concerns inverse problems in ocean acoustics, in which the point forces/sources of the ocean seafloor are determined from acoustic pressure measurements on an array of hydrophones, see Collins and Kuperman (1994).

The above practical applications can be viewed in an unified mathematical way as inverse force problems for the hyperbolic wave equation

$$u_{tt} - \mathcal{L}u = F(x, t, u, u_t, \nabla u),$$

where the operator $\mathcal{L} = \nabla^2$ is the Laplacian for homogeneous media, and $\mathcal{L} = c(x)\nabla^2$ or $\mathcal{L} = \nabla \cdot (\mu(x)\nabla)$ for inhomogeneous media with positive physical properties $c(x)$ or $\mu(x)$,

see Chow and Zou (2014), and $u(x,t)$ and $F(x,t,u,u_t,\nabla u)$ are unknown displacement and forcing term that need to be identified from prescribed initial and Cauchy, i.e. both Dirichlet and Neumann, boundary data.

The linear case when the force $F(x)$ depends only on the space variable x was investigated in some detail both theoretically in Cannon and Dunninger (1970), Klibanov (1992), Engl *et al.* (1994), Yamamoto (1995), and recently, numerically in Hussein and Lesnic (2014, 2016). Also, the purely nonlinear case when the force $F(u)$ depends only on the displacement u, was investigated in Cannon and DuChateau (1983). More recently, inverse coefficient identification problems in which the force expresses as $F(x,u,u_t,\nabla u) = Q_0(x)u + Q_1(x)u_t + Q_2(x)\cdot\nabla u$, with unknown space-dependent coefficients $Q_0(x)$, $Q_1(x)$ and/or $Q_2(x)$, have been the point of interest of some theoretical studies, see Liu and Triggiani (2011, 2013) and Badouin *et al.* (2013). In these studies, the powerful technique of Carleman estimates was employed, see Bukhgeim and Klibanov (1981), Beilina and Klibanov (2012), Klibanov (1992, 2013), and Bellassoued and Yamamoto (2017). It is the pupose of this paper to make new mathematical and numerical contribution along the lines of these nonlinear space-dependent coefficient identification problems for the wave equation.

The plan of the paper is as follows. In Section 2, we give the general setup of the inverse coefficient identification problems (ICIPs) under investigation with particular analysis performed in Section 3. The uniqueness and conditional Lipschitz-type stability of recovering the potential coefficient $Q_0(x)$ is known to hold in certain regular spaces of functions under the assumption of a non-zero initial displacement, as reviewed in Section 3.1, but similar results for recovering the damping coefficient $Q_1(x)$ are not so well-documented. Therefore, subsection 3.2 is devoted to proving these new uniqueness and conditional Lipschitz-type stability results given by Theorem 4 concerning the recovery of the space-dependent damping coefficient. The proof is based on Carleman estimates for the wave equation with forcing terms and approprite extensions of solutions and coefficients to the negative time interval. The analysis requires non-zero initial velocity being prescribed, which may be a practical limitation but this condition is essential for the applicability of the method of Carleman estimates because we must choose/control an initial velocity whose sign is the same everywhere in the closure of the space domain. However, if we change many times the initial displacement or velocity so as the union of their supports covers the closure of the space domain, then the set of all corresponding observation data can yield the same uniqueness and stability results of Theorems 1-4.

After theoretical analysis, Sections 4 and 5 describe the numerical methods used for solving the direct and inverse problems based on the finite difference discretisation and nonlinear contrained minimization using the MATLAB toolbox routine *lsqnonlin*. Section 6 presents and discusses numerical results for the three ICIPs that are investigated. Various features of the investigation include the case of partial Cauchy data, inversion of data contaminated with noise and regularization. Finally, Section 7 presents the conclusions of the study and directions for possible future work.

2 Mathematical formulation

Consider a medium occupying a bounded region Ω in $\mathbb{R}^n$, $n = 1, 2, 3$, with a sufficiently smooth boundary $\partial\Omega$, e.g. of class C^2. Throughout this paper, we assume that $n = 1, 2, 3$. For the case of higher dimensions, $n > 3$, we can argue similarly but we have to assume more regularity of solutions, and we do not discuss it here. Define the space-time cylinder

$Q_T = \Omega \times (0,T)$, where $T > 0$. We wish to find the displacement $u(x,t)$ and the spacewise dependent coefficients $Q_0(x)$ and/or $Q_1(x)$ of the lower-order terms in the hyperbolic wave equation

$$u_{tt} = \nabla^2 u + Q_0(x)u + Q_1(x)u_t \quad \text{in} \quad Q_T. \tag{1}$$

In equation (1), Q_0 is called the potential coefficient, whilst Q_1 is called the damping coefficient. In principle, we could add the extra term $Q_2(x) \cdot \nabla u$ with known or unknown vector coefficient $Q_2(x)$ to the right-hand side of (1), see Liu and Triggiani (2011, 2013), but this additional extension will be investigated in a separate work.

The initial conditions are

$$u(x,0) = \varphi(x), \quad x \in \Omega, \tag{2}$$

$$u_t(x,0) = \psi(x), \quad x \in \Omega, \tag{3}$$

where $\varphi(x)$ and $\psi(x)$ represent the initial displacement and velocity, respectively. On the boundary we can prescribe Dirichlet, Neumann, Robin or mixed boundary conditions.

Let us consider, Neumann boundary conditions being prescribed, namely,

$$\frac{\partial u}{\partial \nu}(x,t) = q(x,t), \quad (x,t) \in \partial\Omega \times (0,T), \tag{4}$$

where q is a given function.

If the functions Q_0 and Q_1 are given, then equations (1)-(4) form a direct well-posed problem. However, if some of the functions Q_0 and/or Q_1 cannot be directly observed they hence become unknown and then clearly, the above set of equations is not sufficient to determine uniquely the solution of the so-generated ICIP. In order to compensate for this non-uniqueness, we consider the additional measurement given by the Dirichlet boundary data,

$$u(x,t) = P(x,t), \quad (x,t) \in \partial\Omega \times (0,T), \tag{5}$$

where P is a prescribed boundary displacement. We can also consider the case when the boundary displacement Dirichlet data (5) is being prescribed and it is the flux tension Neumann data (4) which is being measured.

Note that the unknowns $Q_0(x)$ and $Q_1(x)$ are interior quantities depending on the space variable $x \in \Omega \subset \mathbb{R}^n$, whilst the additional measurement (5) is a boundary quantity depending on $(x,t) \in \partial\Omega \times (0,T)$.

2.1 Preliminaries and notations

For the definitions and notations of concepts related to classical spaces of functional analysis, see Adams (1978) and Lions and Magenes (1972). Also denote by

$$\text{diam}(\Omega) := \min_{x \in \overline{\Omega}} \max_{y \in \overline{\Omega}} |x - y| \tag{6}$$

the diameter of the bounded domain $\Omega \subset \mathbb{R}^n$, $n \geq 1$. Let ν be the outward unit normal to the boundary $\partial\Omega$ and, for any fixed $\mathcal{M} > 0$, denote the admissible set for the coefficient Q_0 as

$$\mathcal{U}_{\mathcal{M}} := \{Q \in W^{1,\infty}(\Omega);\ \big|\big|Q\big|\big|_{W^{1,\infty}(\Omega)} \leq \mathcal{M}\}, \quad L^{\infty}_{\mathcal{M}} := \{Q \in L^{\infty}(\Omega);\ \big|\big|Q\big|\big|_{L^{\infty}(\Omega)} \leq \mathcal{M}\}. \tag{7}$$

In the next section, we analyse more closely the uniqueness of solution of the ICIP's associated to equations (1)-(5).

3 Mathematical analysis

In this section, the discussion is divided into two subsections 3.1 and 3.2 with respect to the three inverse problems generated when $Q_0(x)$, or $Q_1(x)$, or $Q_0(x)$ and $Q_1(x)$ is/are unknown, respectively.

3.1 Unknown coefficient $Q_0(x)$

In this section, we find it useful to review the state-of-the art in the case when the potential $Q_0(x)$ is the unknown coefficient, whilst $Q_1(x)$ is known and, for simplicity, taken to be zero. In this case, equation (1) simplifies to

$$u_{tt} = \nabla^2 u + Q_0(x)u \quad \text{in} \quad Q_T. \tag{8}$$

Before we state the global uniqueness and Lipschitz stability in determining the coefficient $Q_0(x)$, it is useful to mention the well-posedness of the associated direct problem, which can be proved by standard methods, see Lions and Magenes (1972) and Lemma 2.2 of Imanuvilov and Yamamoto (2001a).

Lemma 1.
Assume that $q = 0$, i.e. the Neumann boundary condition (4) *is homogenous,*

$$\frac{\partial u}{\partial \nu}(x,t) = 0, \quad (x,t) \in \partial\Omega \times (0,T), \tag{9}$$

and that the compatibility conditions

$$\varphi \in \left\{ \varphi \in H^3(\Omega); \left.\frac{\partial \varphi}{\partial \nu}\right|_{\partial\Omega} = 0 \right\}, \quad \psi \in \left\{ \psi \in H^2(\Omega); \left.\frac{\partial \psi}{\partial \nu}\right|_{\partial\Omega} = 0 \right\} \tag{10}$$

are satisfied. Assume also that $Q_0 \in \mathcal{U}_{\mathcal{M}}$ for some $\mathcal{M} > 0$ is known. Then the direct problem (2), (3), (8) *and* (9) *is well-posed in the sense that there exists a unique solution*

$$u \in C([0,T]; H^3(\Omega)) \cap C^1([0,T]; H^2(\Omega)) \cap C^2([0,T]; H^1(\Omega)) \tag{11}$$

and furthermore, this solution satisfies the stability estimate

$$||u||_{C([0,T];H^3(\Omega))} + ||u||_{C^1([0,T];H^2(\Omega))} + ||u||_{C^2([0,T];H^1(\Omega))} \leq C(||\varphi||_{H^3(\Omega)} + ||\psi||_{H^2(\Omega)}), \tag{12}$$

for some positive constant $C = C(\Omega, T, \mathcal{M})$.

Previously, Sun (1990) showed that if the initial conditions (2) and (3) are homogeneous then the Neumann to Dirichlet map in certain function spaces continuously determine the potential function $Q_0(x)$ in (8), but this seems to assume too much information. Indeed, with much less information, for the inverse problem (2), (3), (5), (8) and (9) we have the following global uniqueness and Lipschitz stability result due to Imanuvilov and Yamamoto (2001a).

Theorem 1. (see Theorem 1.1 of Imanuvilov and Yamamoto (2001a))
Let $T >$ diam(Ω) and assume that conditions (10) *are satisfied and that*

$$|\varphi(x)| \geq \varphi_0 > 0, \quad \forall x \in \overline{\Omega}, \tag{13}$$

for some $\varphi_0 > 0$. Let u_1 and u_2 be the unique solutions of the direct problem (2), (3), (8) *and* (9) *corresponding to two arbitrary coefficients $Q_0^{(1)}$ and $Q_0^{(2)}$ in $\mathcal{U}_{\mathcal{M}}$ for some fixed $\mathcal{M} > 0$. This makes sense according to Lemma 1 and denote by $P_i := u_i|_{\partial\Omega\times(0,T)}$ the corresponding Dirichlet boundary values of u_i for $i = 1, 2$. Then, there exists a positive constant $C = C(\Omega, T, \mathcal{M}, \varphi, \psi)$ such that the following Lipschitz stability estimate holds:*

$$\left|\left|Q_0^{(1)} - Q_0^{(2)}\right|\right|_{L^2(\Omega)} \leq C\left\|\frac{\partial P_1}{\partial t} - \frac{\partial P_2}{\partial t}\right\|_{H^1(\partial\Omega\times(0,T))}. \tag{14}$$

We can also have the Dirichlet problem, see Yamamoto (1999) and Baudouin *et al.* (2013). First, the corresponding direct problem is well-posed, as given by the following lemma.

Lemma 2. (see Chapter 1 of Lions (1988), Chapter 3 of Lions and Magenes (1972), Lemmas 6-8 of Yamamoto (1999) and Lemma 1 of Baudouin (2011))
(a) Assume that $Q_0 \in L^\infty(\Omega)$ is given,

$$\varphi \in L^2(\Omega), \quad \psi \in H^{-1}(\Omega), \quad P \in L^2(\partial\Omega \times (0,T)), \tag{15}$$

and that the compatibility condition

$$P(x,0) = \varphi(x), \quad x \in \partial\Omega \tag{16}$$

is satisfied. Then the direct problem (2), (3), (5) *and* (8) *is well-posed in the sense that there exists a unique solution*

$$u \in C([0,T]; L^2(\Omega)) \cap C^1([0,T]; H^{-1}(\Omega)), \tag{17}$$

and furthermore, this solution satisfies the stability estimate

$$\|u\|_{L^\infty(0,T;L^2(\Omega))} \leq C(\|\varphi\|_{L^2(\Omega)} + \|\psi\|_{H^{-1}(\Omega)} + \|P\|_{L^2(\partial\Omega\times(0,T))}), \tag{18}$$

for some positive constant $C = C(\Omega, T, Q_0)$.
(b) Assume that $P = 0$, i.e. the Dirichlet boundary condition (5) *is homogenous,*

$$u(x,t) = 0, \quad (x,t) \in \partial\Omega \times (0,T), \tag{19}$$

and that $Q_0 \in L^\infty_{\mathcal{M}}$ for some $\mathcal{M} > 0$ is known. Assume also that

$$\varphi \in H_0^1(\Omega), \quad \psi \in L^2(\Omega). \tag{20}$$

Then the direct problem (2), (3), (8) *and* (19) *is well-posed in the sense that there exists a unique solution*

$$u \in C([0,T]; H_0^1(\Omega)) \cap C^1([0,T]; L^2(\Omega)), \tag{21}$$

and furthermore, we have the stability estimates

$$\|u_t(\cdot,t)\|^2_{L^2(\Omega)} + \|\nabla u(\cdot,t)\|^2_{(L^2(\Omega))^n} \leq C(\|\varphi\|^2_{H_0^1(\Omega)} + \|\psi\|^2_{L^2(\Omega)}), \quad t \in [0,T], \tag{22}$$

$$\left\| \frac{\partial u}{\partial \nu} \right\|_{L^2(\partial\Omega\times(0,T))} \leq C(\|\varphi\|_{H_0^1(\Omega)} + \|\psi\|_{L^2(\Omega)}), \tag{23}$$

for some positive constant $C = C(\Omega, T, \mathcal{M})$.

If instead of conditions (20) *we have the stronger assumptions*

$$\varphi \in H^2(\Omega) \cap H_0^1(\Omega), \quad \psi \in H_0^1(\Omega), \tag{24}$$

then, instead of (23) *we have the estimate*

$$\left\| \frac{\partial u}{\partial \nu} \right\|_{H^1(0,T;L^2(\partial\Omega))} \leq C(\|\varphi\|_{H^2(\Omega)} + \|\psi\|_{H_0^1(\Omega)}). \tag{25}$$

For the inverse problem (2)-(5) and (8) we have the following uniqueness and Lipschitz stability result due to Yamamoto (1999).

Theorem 2. (see Theorems 2 and 4 of Yamamoto (1999))
Let $T > \operatorname{diam}(\Omega)$ *and assume that*

$$\varphi \in H^1(\Omega), \quad \psi \in L^2(\Omega), \quad P \in L^2(\partial\Omega \times (0,T)). \tag{26}$$

Also assume that

$$|\varphi(x)| \geq \varphi_0 > 0, \quad a.e. \quad x \in \overline{\Omega}, \tag{27}$$

for some constant $\varphi_0 > 0$. *Let* u_1 *and* u_2 *be the unique solutions of the direct problem* (2), (3), (5) *and* (8) *corresponding to two arbitrary potentials* $Q_0^{(1)}$ *and* $Q_0^{(2)}$ *in* $L^\infty_{\mathcal{M}}$ *for some fixed* $\mathcal{M} > 0$. *Denote by* $q_i := \frac{\partial u_i}{\partial \nu}|_{\partial\Omega\times(0,T)}$ *the corresponding Neumann boundary values of* u_i *for* $i = 1, 2$. *Further, assume that*

$$u_1 \text{ or } u_2 \in W^{3,\infty}(Q_T). \tag{28}$$

Then $q_1 = q_2$ *implies* $Q_0^{(1)} = Q_0^{(2)}$ *and* $u_1 = u_2$. *Furthermore, assuming that* $Q_0^{(2)} \in L^\infty(\Omega)$ *is given and that*

$$\|u_1\|_{W^{3,\infty}(\Omega\times(0,T))} \leq \mathcal{M}, \tag{29}$$

then there exists a positive constant $C = C(\Omega, T, \varphi, \psi, \mathcal{M}, Q_0^{(2)})$ *such that the following Lipschitz stability holds:*

$$C^{-1}\big|\big|Q_0^{(1)} - Q_0^{(2)}\big|\big|_{L^2(\Omega)} \leq \big|\big|q_1 - q_2\big|\big|_{H^1(0,T;L^2(\partial\Omega))} \leq C\big|\big|Q_0^{(1)} - Q_0^{(2)}\big|\big|_{L^2(\Omega)}, \tag{30}$$

for all $Q_0^{(1)} \in L^\infty_{\mathcal{M}}$.

In certain applications, the flux (4) can only be measured on a portion $\Gamma_0 \subset \partial\Omega$, namely,

$$\frac{\partial u}{\partial \nu}(x,t) = q(x,t), \quad (x,t) \in \Gamma_0 \times (0,T). \tag{31}$$

In this case, we further need the geometrical assumptions that, see Klibanov (1992, 2013) and Beilina and Klibanov (2012),

$$\exists x_0 \notin \overline{\Omega} \text{ such that } \{x \in \partial\Omega | (x - x_0) \cdot \nu(x) \geq 0\} \subset \Gamma_0, \tag{32}$$

$$T > \sup_{x \in \Omega} |x - x_0|, \tag{33}$$

in order for the Carleman estimates to be applicable. Then we still have the local Lipschitz stability estimates (30) for $q_1 - q_2 \in H^1(0,T;L^2(\Gamma_0))$, assuming that $Q_0^{(2)} \in L^\infty_{\mathcal{M}}$ and

$$u_2 \in H^1(0,T;L^\infty(\Omega)), \tag{34}$$

instead of (29), see Theorem 1 of Baudouin (2011). Remark that since $W^3(\Omega \times (0,T)) \subset H^1(0,T;L^\infty(\Omega))$ assumption (34) is weaker than (29). Also, condition (34) can be guaranteed uniformly for $Q_0^{(2)} \in L^\infty_{\mathcal{M}}$ if the data (2), (3) and (5) have the higher regularity

$$\varphi \in H^2(\Omega), \quad \psi \in H^1(\Omega), \quad P \in H^2(0,T;H^2(\Omega)), \tag{35}$$

and satisfy the compatibility conditions (16) and

$$\partial_t P(x,0) = \psi(x), \quad x \in \partial\Omega, \tag{36}$$

see Remark 1 of Baudouin (2011).

3.2 Unknown coefficient $Q_1(x)$

In this section, we investigate the case when the damping term $Q_1(x)$ is the unknown coefficient, whilst $Q_0(x)$ is known and, for simplicity, taken to be zero. In this case, equation (1) simplifies to

$$u_{tt} = \nabla^2 u + Q_1(x) u_t \quad \text{in} \quad Q_T. \tag{37}$$

Then for the inverse problem (2), (3), (5), (31) and (37) we have the following uniqueness result due to Bukhgeim et al. (2001).

Theorem 3. (see Theorem 2 of Bukhgeim et al. (2001))
Let the assumptions (26)*,* (32) *and* (33) *be satisfied and also assume that*

$$|\psi(x)| \geq \psi_0 > 0, \quad a.e. \quad x \in \overline{\Omega} \tag{38}$$

for some constant $\psi_0 > 0$*. Let* u_1 *and* u_2 *be the unique solutions of the direct problems* (2)*,* (3)*,* (5) *and* (37) *corresponding to two arbitrary damping coefficients* $Q_1^{(1)}$ *and* $Q_1^{(2)}$ *in* $L^\infty(\Omega)$ *and assume that condition* (28) *is satisfied. Denote by* $q_i := \frac{\partial u_i}{\partial \nu}|_{\Gamma_0 \times (0,T)}$ *the corresponding Neumann boundary values of* u_i *on* $\Gamma_0 \times (0,T)$ *for* $i = 1,2$*. Then* $q_1 = q_2$ *implies* $Q_1^{(1)} = Q_1^{(2)}$ *and* $u_1 = u_2$*.*

The proof in Bukhgeim et al. (2001) is long and somewhat complicated. In what follows, we give a simpler proof as well as establish the Lipschitz stability of the inverse problem by

using similar arguments to those employed by Imanuvilov and Yamamoto (2001b). We also can assume without loss of generality that

$$\{x \in \partial\Omega | (x - x_0) \cdot \nu(x) \geq 0\} = \Gamma_0, \tag{39}$$

instead of (32).

Theorem 4.
Let the assumptions (26), (33), (38) *and* (39) *be satisfied. Let* u_1 *and* u_2 *be the unique solutions of the direct problems* (2), (3), (5) *and* (37) *corresponding to two arbitrary damping coefficients* $Q_1^{(1)}$ *and* $Q_1^{(2)}$ *in* $L^\infty_{\mathcal{M}}$ *for some fixed* $\mathcal{M} > 0$. *Further, assume that*

$$u_i \in H^3(0,T;L^2(\Omega)) \cap H^2(0,T;H^2(\Omega)), \tag{40}$$

$$\|u_i\|_{H^3(0,T;L^2(\Omega))} \leq \mathcal{M}, \tag{41}$$

$$\left\| \frac{\partial u_i}{\partial t} \right\|_{L^\infty(\Omega\times(0,T))} \leq \mathcal{M}, \tag{42}$$

for $i = 1, 2$. *Denote by* $q_i := \frac{\partial u_i}{\partial \nu}|_{\Gamma_0\times(0,T)}$. *Then there exists a positive constant* $C = C(\Omega, T, \mathcal{M}, \varphi, \psi, h)$ *such that the following Lipschitz stability estimate holds:*

$$\left|\left|Q_1^{(1)} - Q_1^{(2)}\right|\right|_{L^2(\Omega)} \leq C \left|\left|q_1 - q_2\right|\right|_{H^1(0,T;L^2(\Gamma_0))}. \tag{43}$$

Proof. Denoting by $U := u_1 - u_2$, $f(x) = Q_1^{(1)}(x) - Q_1^{(2)}(x)$ and $R = \partial_t u_2$, we immediately obtain from (2), (3), (5) and (37) the following system:

$$U_{tt} = \nabla^2 U + Q_1^1(x) U_t + f(x) R(x,t) \quad \text{in} \quad Q_T, \tag{44}$$

$$U(x,0) = U_t(x,0) = 0, \quad x \in \Omega, \tag{45}$$

$$U(x,t) = 0, \quad (x,t) \in \partial\Omega \times (0,T). \tag{46}$$

We then have an inverse linear space-dependent force problem of determining $f(x)$ from the Neumann data measurement

$$\frac{\partial U}{\partial \nu}(x,t) = q_1(x,t) - q_2(x,t),, \quad (x,t) \in \Gamma_0 \times (0,T). \tag{47}$$

Remark that condition (38) implies

$$R(x,0) \neq 0, \quad \text{a.e.} \quad x \in \overline{\Omega}. \tag{48}$$

and condition (40) yields that

$$U \in H^3(0,T;L^2(\Omega)) \cap H^2(0,T;H^2(\Omega)). \tag{49}$$

As $n = 1, 2, 3$ and from the Sobolev embedding theorem $H^2(\Omega) \subset C(\overline{\Omega})$, condition (40) for u_2 implies that

$$R \in H^1(0, T; L^\infty(\Omega)) \quad \text{and} \quad R, \partial_t R \in L^\infty(Q_T). \tag{50}$$

The Lipschitz stability condition (43) that we have to prove recasts as

$$\|f\|_{L^2(\Omega)} \leq C \|\partial_\nu U\|_{H^1(0,T;L^2(\Gamma_0))}. \tag{51}$$

First, we make the even extension of U to $(-T, 0)$ keeping the hyperbolicity of the wave equation (44). We extend U, $Q_1^{(1)}$ and R to the time interval $(-T, T)$ by

$$U(x,t) = \begin{cases} U(x,t), & (x,t) \in \Omega \times [0,T) \\ U(x,-t), & (x,t) \in \Omega \times (-T,0) \end{cases} \tag{52}$$

$$Q(x,t) = \begin{cases} Q_1^{(1)}(x), & (x,t) \in \Omega \times [0,T) \\ -Q_1^{(1)}(x), & (x,t) \in \Omega \times (-T,0) \end{cases} \tag{53}$$

$$R(x,t) = \begin{cases} R(x,t), & (x,t) \in \Omega \times [0,T) \\ R(x,-t), & (x,t) \in \Omega \times (-T,0) \end{cases} \tag{54}$$

Then from (45) and (52) one can easily observe that

$$\partial_t U(x,t) = \begin{cases} \partial_t U(x,t), & (x,t) \in \Omega \times [0,T) \\ -\partial_t U(x,-t), & (x,t) \in \Omega \times (-T,0) \end{cases} \tag{55}$$

$$\partial_t^2 U(x,t) = \begin{cases} \partial_t^2 U(x,t), & (x,t) \in \Omega \times [0,T) \\ \partial_t^2 U(x,-t), & (x,t) \in \Omega \times (-T,0) \end{cases} \tag{56}$$

and thus (49) has been extended to

$$U \in H^3(-T, T; L^2(\Omega)) \cap H^2(-T, T; H^2(\Omega)). \tag{57}$$

Also from (54) we have extended (50) to

$$R \in H^1(-T, T; L^\infty(\Omega)) \quad \text{and} \quad \partial_t R \in L^\infty(\Omega \times (-T, T)). \tag{58}$$

Thus the whole system (44)-(46) has been extended to

$$U_{tt}(x,t) = \nabla^2 U(x,t) + Q(x,t) U_t(x,t) + f(x) R(x,t), \quad (x,t) \in \Omega \times (-T, T), \tag{59}$$

$$U(x,0) = U_t(x,0) = 0, \quad x \in \Omega, \tag{60}$$

$$U(x,t) = 0, \quad (x,t) \in \partial\Omega \times (-T, T). \tag{61}$$

First, we have a Carleman estimate, see Imanuvilov and Yamamoto (2001b) and Bellassoued and Yamamoto (2014), given in the following lemma.

Lemma 3.
Let $Q \in L^\infty(Q_T)$, $x_0 \notin \overline{\Omega}$, $\beta \in (0,1)$ and $\lambda > 0$ be sufficiently large. Set

$$b(x,t) = |x - x_0|^2 - \beta t^2, \quad a(x,t) = e^{\lambda b(x,t)}. \tag{62}$$

Then there exists constants $s_0 > 0$ and $C > 0$ such that

$$\int_{Q_T} (s|\nabla_{x,t} V|^2 + s^3 V^2) e^{2sa(x,t)} dxdt \leq C \int_{Q_T} |\mathcal{P}(V)|^2 e^{2sa(x,t)} dxdt$$
$$+C \int_{-T}^{T} \int_{\Gamma_0} s|\partial_\nu V|^2 e^{2sa(x,t)} dS(x)dt \tag{63}$$

for all $s \geq s_0$ and $V \in H^2(\Omega \times (-T,T))$ satisfying

$$V|_{\partial\Omega \times (-T,T)} = 0 \quad \text{and} \quad V(x, \pm T) = V_t(x, \pm T) = 0, \quad x \in \Omega. \tag{64}$$

In (63), we used the notation

$$\mathcal{P}(V) := V_{tt} - \nabla^2 V - Q(x,t) V_t. \tag{65}$$

Second, we verify that

$$\partial_t (Q(x,t) \partial_t U(x,t)) = Q(x,t) \partial_t^2 U(x,t) \quad \text{in} \quad L^2(\Omega \times (-T,T)), \tag{66}$$

where we have denoted $\partial_t^2 U(x,t) = U_{tt}(x,t)$. Indeed, let $x \in \overline{\Omega}$ be arbitrarily fixed. Then for any $g \in C_0^\infty(-T,T)$, from (53) and (55), we have (using $g(\pm T) = 0$)

$$-\int_{-T}^{T} \partial_t (Q(x,t) \partial_t U(x,t)) g(t) dt = \int_{-T}^{T} Q(x,t) \partial_t U(x,t) g'(t) dt$$
$$= \left(\int_0^T + \int_{-T}^0 \right) Q(x,t) \partial_t U(x,t) g'(t) dt = \int_0^T Q_1^{(1)}(x) \partial_t U(x,t) g'(t) dt$$
$$+ \int_{-T}^0 Q_1^{(1)}(x) \partial_t U(x,-t) g'(t) dt. \tag{67}$$

From (49) we have that $\partial_t U \in H^2(0,T; L^2(\Omega))$ and integration by parts yields

$$\begin{aligned} \int_{-T}^{T} Q(x,t) \partial_t U(x,t) g'(t) dt &= \int_0^T Q_1^{(1)}(x) \partial_t U(x,t) g'(t) dt + \int_{-T}^0 Q_1^{(1)}(x) \partial_t U(x,-t) g'(t) dt \\ &= Q_1^{(1)}(x) \partial_t U(x,t) g(t) dt \Big|_{t=0}^{t=T} + Q_1^{(1)}(x) \partial_t U(x,-t) g(t) \Big|_{t=-T}^{t=0} \\ &\quad - \int_0^T Q_1^{(1)}(x) \partial_t^2 U(x,t) g(t) dt + \int_{-T}^0 Q_1^{(1)}(x) \partial_t^2 U(x,-t) g(t) dt. \end{aligned} \tag{68}$$

By $g(\pm T) = 0$ and equations (45), (53) and (56), we obtain that the right hand-side of (68) is equal to $-\int_{-T}^{T} Q(x,t) \partial_t^2 U(x,t) g(t) dt$. Therefore, the identity (66) is satisfied in the weak sense in $L^2(Q_T)$.

In view of (66), by taking the t-derivative in (59)-(61) we obtain

$$\partial_t^2(\partial_t U)(x,t) = \nabla^2(\partial_t U)(x,t) + Q(x,t)\partial_t(\partial_t U(x,t)) + f(x)\partial_t R(x,t), \\ (x,t) \in \Omega \times (-T,T), \tag{69}$$

$$\partial_t U(x,0) = 0, \quad \partial_t(\partial_t U)(x,0) = f(x)R(x,0), \quad x \in \Omega, \tag{70}$$

$$\partial_t U\Big|_{\partial\Omega\times(-T,T)} = 0. \tag{71}$$

From (33) and $x_0 \notin \overline{\Omega}$, we can choose $\beta \in (0,1)$ such that

$$T > \frac{1}{\sqrt{\beta}} \sup_{x\in\Omega} |x - x_0|. \tag{72}$$

Then from (62) we obtain

$$b(x, \pm T) < 0, \quad b(x,0) > 0, \quad x \in \overline{\Omega}. \tag{73}$$

Then we can choose a sufficiently small $\delta > 0$ such that

$$\begin{cases} b(x,t) < -\delta, & x \in \overline{\Omega}, \quad |T-t| < 2\delta \quad \text{or} \quad |t+T| < 2\delta, \\ b(x,t) > \delta, & x \in \overline{\Omega}, \quad |t| < 2\delta. \end{cases} \tag{74}$$

This implies that

$$\begin{cases} a(x,t) < e^{-\lambda\delta} < 1, & x \in \overline{\Omega}, \quad |T-t| < 2\delta \quad \text{or} \quad |t+T| < 2\delta, \\ a(x,t) > e^{\lambda\delta} > 1, & x \in \overline{\Omega}, \quad |t| < 2\delta. \end{cases} \tag{75}$$

We now define a cut-off function $\mathcal{X} \in C^\infty(\mathbb{R})$ such that $0 \le \mathcal{X} \le 1$ and

$$\mathcal{X}(t) = \begin{cases} 0, & |T-t| < \delta \quad \text{or} \quad |t+T| < \delta, \\ 1, & |t| < T - 2\delta. \end{cases} \tag{76}$$

Set

$$z := (\partial_t U)\mathcal{X}e^{sa} \in H^2(-T,T;L^2(\Omega)) \cap H^1(-T,T;H^2(\Omega)) \tag{77}$$

and

$$w := (\partial_t U)\mathcal{X} \in H^2(-T,T;L^2(\Omega)) \cap H^1(-T,T;H^2(\Omega)). \tag{78}$$

Using (65) and (69) by direct calculation we obtain that

$$\mathcal{P}z = (\partial_t R) f \mathcal{X} e^{sa} + 2s(-\nabla a \cdot \nabla z + (\partial_t a)\partial_t z) + s^2(|\nabla a|^2 - (\partial_t a)^2)z \\ + s((\partial_t^2 - \nabla^2 - Q\partial_t)a)z + e^{sa}(\partial_t \mathcal{X})(2\partial_t^2 U - Q\partial_t U) + e^{sa}(\partial_t^2 \mathcal{X})\partial_t U \quad \text{in} \quad Q_T, \tag{79}$$

and

$$\mathcal{P}w = (\partial_t R) f \mathcal{X} + (\partial_t \mathcal{X})(2\partial_t^2 U - Q\partial_t U) + (\partial_t^2 \mathcal{X})\partial_t U \quad \text{in} \quad Q_T. \tag{80}$$

Applying Lemma 3 to (80) and noting that $w(x,\pm T)=\partial_t w(x,\pm T)=0$, we have

$$\int_{Q_T}(s|\nabla_{x,t}U|^2+s^3U^2)e^{2sa(x,t)}dxdt\le C\int_{Q_T}|(\partial_t R)f\mathcal{X}|^2e^{2sa(x,t)}dxdt$$
$$+C\int_{Q_T}(|\partial_t\mathcal{X}|^2|2\partial_t^2U-Q\partial_tU|^2+|(\partial_t^2\mathcal{X})\partial_tU|^2)e^{2sa(x,t)}dxdt+CD^2e^{Cs} \tag{81}$$

for sufficiently large $s>0$, where

$$D^2:=\|\partial_\nu U\|^2_{H^1(-T,T;L^2(\Gamma_0))}=2\|\partial_\nu U\|^2_{H^1(0,T;L^2(\Gamma_0))}. \tag{82}$$

Throughout the proof, C denotes an arbitrary generic positive constant independent of s. From (76) it follows that the second integral in the right-hand side of (81) does not vanish only in $t\in(-T+\delta,-T+2\delta)\cup(T-2\delta,T-\delta)$. Therefore, (52), (55), (56) and (75) yield

$$C\int_{Q_T}(|\partial_t\mathcal{X}|^2|2\partial_t^2U-Q\partial_tU|^2+|(\partial_t^2\mathcal{X})\partial_tU|^2)e^{2sa(x,t)}dxdt$$
$$\le Ce^{2s}\|U\|^2_{H^2(-T,T;L^2(\Omega))}\le 2Ce^{2s}\|U\|^2_{H^2(0,T;L^2(\Omega))}=:Ce^{2s}\mathcal{M}_1^2, \tag{83}$$

where $\mathcal{M}_1:=\|U\|_{H^2(0,T;L^2(\Omega))}$. Hence from (81) and (83) we obtain

$$\int_{Q_T}(s|\nabla_{x,t}w|^2+s^3w^2)e^{2sa(x,t)}dxdt\le C\int_{Q_T}|(\partial_t R)f|^2e^{2sa(x,t)}dxdt+Ce^{2s}\mathcal{M}_1^2+CD^2e^{Cs} \tag{84}$$

for sufficiently large $s>0$.

Next we multiply (79) by $\partial_t z(x,t)$ for $t\in(0,T)$ and integrate with respect to $x\in\Omega$. Then, for some functions $\underline{A}\in(L^\infty(\Omega))^{n+1}$, $b_0,b_1\in L^\infty(Q_T)$, using (65) we have

$$\int_\Omega(\partial_t^2z)\partial_tzdx-\int_\Omega(\nabla^2z)\partial_tzdx-\int_\Omega Q(x,t)|\partial_tz|^2dx$$
$$=\int_\Omega f\mathcal{X}(\partial_tR)e^{sa(x,t)}\partial_tzdx+s\int_\Omega(\underline{A}(x,t).\nabla_{x,t}z)\partial_tzdx+\int_\Omega(sb_0+s^2b_1)z\partial_tzdx$$
$$+\int_\Omega((\partial_t\mathcal{X})(2\partial_t^2U-Q\partial_tU)+(\partial_t^2\mathcal{X})\partial_tU)e^{sa(x,t)}\partial_tzdx,\quad t\in(0,T). \tag{85}$$

From (60), (71), (76) and (77) we have that $z(x,0)=0=z(x,T)=z_t(x,T)$ for $x\in\Omega$ and that $z|_{\partial\Omega\times(0,T)}=0$. Then, by integration by parts we have

$$\int_0^T[\text{left-hand side of (85)}]dt=\int_0^T\left\{\frac{1}{2}\partial_t\left(\int_\Omega|\partial_tz|^2dx\right)-\int_\Omega Q(x,t)|\partial_tz|^2dx\right.$$
$$\left.+\frac{1}{2}\partial_t\left(\int_\Omega|\nabla z|^2dx\right)\right\}dt=-\frac{1}{2}\int_\Omega\left(|\partial_tz(x,0)|^2+|\nabla z(x,0)|^2\right)dx$$
$$-\int_0^T\int_\Omega Q(x,t)|\partial_tz(x,t)|^2dxdt. \tag{86}$$

Since from (77) we have $\partial_tz=(\partial_t^2U)\mathcal{X}e^{sa}+(\partial_tU)(\partial_t(\mathcal{X}e^{sa}))$ and using (60), from (59), (70) and (76) we have

$$\partial_tz(x,0)=(\partial_t^2U)(x,0)\mathcal{X}(0)e^{sa(x,0)}=f(x)R(x,0)e^{sa(x,0)},\quad|\nabla z(x,0)|^2=0,\ x\in\Omega.$$

Consequently, (86) implies that

$$\int_0^T [\text{left-hand side of (85)}]dt = -\frac{1}{2}\int_\Omega |f(x)|^2 |R(x,0)|^2 e^{2sa(x,0)}dx$$
$$-\int_{Q_T} Q(x,t)|\partial_t z(x,t)|^2 dxdt. \tag{87}$$

On the other hand, by the Cauchy-Schwarz inequality, similarly to (83), we obtain

$$\left|\int_0^T [\text{right-hand side of (85)}]dt\right| \le \int_{Q_T} |f\mathcal{X}(\partial_t R)e^{sa}\partial_t z|dxdt + Cs\int_{Q_T} |\nabla_{x,t} z||\partial_t z|dxdt$$
$$+Cs^2\int_{Q_T} |z\partial_t z|dxdt + C\int_{Q_T}\left\{|\partial_t \mathcal{X}|(|\partial_t^2 U| + |\partial_t U|) + |\partial_t^2 \mathcal{X}||\partial_t U|\right\}|\partial_t z|e^{sa}dxdt$$
$$\le C\int_{Q_T} |f|^2 e^{2sa}dxdt + C\int_{Q_T}(s|\nabla_{x,t} z|^2 + Cs^3 z^2)dxdt + Ce^{2s}\mathcal{M}_1^2, \tag{88}$$

where we have also used that

$$s^2|z\partial_t z| = |(s^{3/2}z)(s^{1/2}\partial_t z)| \le \frac{1}{2}s^3 z^2 + \frac{1}{2}s|\partial_t z|^2 \le \frac{1}{2}s^3 z^2 + \frac{1}{2}s|\nabla_{x,t} z|^2$$

and

$$s|\nabla_{x,t} z||\partial_t z| \le \frac{s}{2}(|\nabla_{x,t} z|^2 + |\partial_t z|^2) \le s|\nabla_{x,t}|^2.$$

By (48), there exists $\delta_0 > 0$ such that $|R(x,0)| \ge \delta_0 > 0$ a.e. $\overline{\Omega}$. Substituting (87) and (88) into (85), we obtain

$$\int_\Omega |f(x)|^2 e^{2sa(x,0)}dx \le C\int_{Q_T} |f(x)|^2 e^{2sa}dxdt + C\int_{Q_T}(s|\nabla_{x,t} z|^2 + s^3 z^2)dxdt + Ce^{2s}\mathcal{M}_1^2,$$

for sufficiently large $s > 0$. Rewritting (84) in terms of $z := we^{sa}$ and substituting into the above inequality result in

$$\int_\Omega |f(x)|^2 e^{2sa(x,0)}dx \le C\int_{Q_T} |f(x)|^2 e^{2sa(x,t)}dxdt + Ce^{2s}\mathcal{M}_1^2 + CD^2 e^{Cs}, \tag{89}$$

for sufficiently large $s > 0$. Here

$$\int_{Q_T} |f(x)|^2 e^{2sa(x,t)}dxdt \le \int_\Omega |f(x)|^2 e^{2sa(x,0)}\left(\int_{-T}^T e^{2s(a(x,t)-a(x,0))}dt\right)dx. \tag{90}$$

Since $a(x,t) - a(x,0) = e^{\lambda|x-x_0|^2}\left(e^{-\lambda\beta t^2} - 1\right) < 0$ if $t \ne 0$, the Lebesgue theorem implies

$$\int_{-T}^T e^{2s(a(x,t)-a(x,0))}dt = o(1) \quad \text{as} \quad s \to \infty.$$

Therefore, by choosing $s > 0$ sufficiently large, equations (89) and (90) imply

$$\frac{1}{2}\int_\Omega |f(x)|^2 e^{2sa(x,0)}dx \le (1 - o(1))\int_\Omega |f(x)|^2 e^{2sa(x,0)}dx \le Ce^{2s}\mathcal{M}_1^2 + CD^2 e^{Cs}. \tag{91}$$

On the other hand, a usual *a priori* estimate for the initial boundary value problem (44)-(46) gives

$$\mathcal{M}_1 = \|U\|_{H^2(0,T;L^2(\Omega))} \le C\|fR\|_{H^1(0,T;L^2(\Omega))} \le C\|f\|_{L^2(\Omega)}. \tag{92}$$

Thus, (91) yields

$$\int_\Omega |f(x)|^2 e^{2sa(x,0)}dx - Ce^{2s}\int_\Omega |f(x)|^2 dx \le CD^2 e^{Cs}, \tag{93}$$

for large $s > 0$. In view of (75), we have

$$e^{2sa(x,0)} > e^{2se^{\lambda\delta}}, \quad x \in \overline{\Omega}$$

and (93) yields

$$(e^{2se^{\lambda\delta}} - Ce^{2s})\|f\|^2_{L^2(\Omega)} \le CD^2 e^{Cs}$$

for large $s > 0$. Since

$$e^{2se^{\lambda\delta}} - Ce^{2s} = e^{2se^{\lambda\delta}}(1 - Ce^{2s(1-e^{\lambda\delta})})$$

and $1 - e^{\lambda\delta} < 0$, choosing $s > 0$ large enough we can obtain that

$$\frac{1}{2}e^{2se^{\lambda\delta}}\|f\|^2_{L^2(\Omega)} \le CD^2 e^{Cs}.$$

This inequality, (47) and (82) together with $f(x) = Q_1^{(1)}(x) - Q_1^{(2)}(x)$ yield the Lipschitz stability estimate (43), as required. This ends the proof of Theorem 4.

As for the simultaneous determination of the potential $Q_0(x)$ and the damping term $Q_1(x)$, see Liu and Triggiani (2011, 2013) for a related (but different) formulation corresponding to the inverse problem (1)-(5) on the time interval $t \in (-T, T)$ but not on $(0, T)$.

4 Numerical solution of the direct problem

In this section, we consider the direct initial Neumann boundary value problem (1)-(4) for simplicity, in one-dimension, i.e. $n = 1$ and $\Omega = (0, L)$ with $L > 0$, when the coefficients $Q_0(x)$, $Q_1(x)$ and $Q_2(x)$ are known and the displacement $u(x, t)$ is to be determined, namely,

$$u_{tt}(x,t) = u_{xx}(x,t) + Q_0(x)u + Q_1(x)u_t + Q_2(x)u_x, \quad (x,t) \in (0,L)\times(0,T], \tag{94}$$

$$u(x,0) = \varphi(x), \quad u_t(x,0) = \psi(x), \quad x \in [0,L], \tag{95}$$

$$-\frac{\partial u}{\partial x}(0,t) = q(0,t) =: q_0(t), \quad \frac{\partial u}{\partial x}(L,t) = q(L,t) =: q_L(t), \quad t \in (0,T]. \tag{96}$$

In the direct problem (94)-(96) of interest is to determine the Dirichlet boundary data (5) at $x = 0$ and $x = L$, namely

$$u(0,t) = P(0,t) =: P_0(t), \quad u(L,t) = P(L,t) =: P_L(t), \quad t \in (0,T]. \tag{97}$$

The discrete form of the problem (1)-(4) is as follows. We divide the solution domain $(0, L) \times (0, T)$ into M and N subintervals of equal space length Δx and time step Δt, where $\Delta x = L/M$ and $\Delta t = T/N$. We denote $u_{i,j} := u(x_i, t_j)$, where $x_i = i\Delta x$, $t_j = j\Delta t$, $Q_{0i} := Q_0(x_i)$, $Q_{1i} := Q_1(x_i)$ and $Q_{i2} := Q_2(x_i)$ for $i = \overline{0, M}$, $j = \overline{0, N}$. Then, a central-difference approximation to equations (94)-(96) at the mesh points $(x_i, t_j) = (i\Delta x, j\Delta t)$ of the rectangular mesh covering the solution domain $(0, L) \times (0, T)$ is, see e.g. Smith (1985),

$$u_{i,j+1} = \frac{r + r_0 Q_{2i}}{1 - r_1 Q_{1i}} u_{i+1,j} + \frac{2 - 2r + (\Delta t)^2 Q_{0i}}{1 - r_1 Q_{1i}} u_{i,j} + \frac{r - r_0 Q_{2i}}{1 - r_1 Q_{1i}} u_{i-1,j} - \frac{1 + r_1 Q_{1i}}{1 - r_1 Q_{1i}} u_{i,j-1}, \quad i = \overline{1, (M-1)}, \quad j = \overline{1, (N-1)}, \tag{98}$$

$$u_{i,0} = \varphi(x_i), \quad i = \overline{0, M}, \quad \frac{u_{i,1} - u_{i,-1}}{2\Delta t} = \psi(x_i), \quad i = \overline{1, (M-1)}, \tag{99}$$

$$-\frac{\partial u}{\partial x}(0, t_j) = -\frac{4u_{1,j} - u_{2,j} - 3u_{0,j}}{2\Delta x} = q_0(t_j),$$
$$\frac{\partial u}{\partial x}(L, t_j) = \frac{3u_{M,j} - 4u_{M-1,j} + u_{M-2,j}}{2\Delta x} = q_L(t_j), \quad j = \overline{1, N}, \tag{100}$$

where $r = (\Delta t)^2/(\Delta x)^2$, $r_0 = (\Delta t)^2/(2\Delta x)$ and $r_1 = \Delta t/2$. Equation (98) represents an explicit finite-difference method (FDM) which is stable if $r \leq 1$, giving approximate values for the solution at mesh points along $t = 2\Delta t, 3\Delta t, ...$, as soon as the solution at the mesh points along $t = \Delta t$ has been determined. Putting $j = 0$ in equation (98) and using (99), we obtain

$$u_{i,1} = \frac{r + r_0 Q_{2i}}{2} \varphi(x_{i+1}) + \frac{2 - 2r + (\Delta t)^2 Q_{0i}}{2} \varphi(x_i) + \frac{r - r_0 Q_{2i}}{2} \varphi(x_{i-1}) + \Delta t(1 + r_1 Q_{1i}) \psi(x_i) \quad i = \overline{1, (M-1)}. \tag{101}$$

The time-marching FDM procedure described above provides the displacement u throughout the solution domain and in particular the Dirichlet data (97) given by

$$u_{0,j} = P_0(t_j), \quad u_{M,j} = P_L(t_j), \quad j = \overline{1, N}. \tag{102}$$

5 Numerical approach to the inverse problems

In the inverse problem stated in Section 2, we wish to determine the solution of unknown $(u(x,t), Q_0(x), Q_1(x))$ by minimizing the nonlinear objective function

$$\mathcal{F}(Q_0, Q_1) = \|u(x, t; Q_0, Q_1) - P(x, t)\|^2_{L^2(\partial\Omega \times (0,T))}. \tag{103}$$

This minimisation is accomplished using the MATLAB optimisation toolbox routine *lsqnonlin* which attempts to find a minimum of a sum of squares, starting from an arbitrary initial guess, subject to constraints. In MATLAB, this routine allows to choose the trust-region-reflective algorithm based on the interior-reflective Newton method, see Coleman and Li (1994), and more details about its generic implementation for minimizing least-squares functionals like (103) can be found in Ito and Liu (2013). Alternatively, one could use the

MATLAB toolbox routine *fmincon* based on the interior point algorithm, but the comparison between *lsqnonlin* and *fmincon* made in Hussein and Lesnic (2016) for a similar minimization problem revealed equal performance in accuracy but for some increase in the computational time in the *fmincon*.

In practice, the additional observation (5) comes from measurement which is inherently contaminated with errors,

$$P^{\epsilon}(x,t) = P(x,t) + \epsilon, \quad (x,t) \in \partial\Omega \times (0,T), \tag{104}$$

where ϵ stands for the amount of noise. In this case, we replace in the objective functional (103) the exact data $P(x,t)$ by the noisy data $P^{\epsilon}(x,t)$.

6 Numerical results and discussion

In all examples in this section we consider, for simplicity, the one-dimensional case, i.e. $n = 1$ and $\Omega = (0, L)$, with $L = T = 1$.

6.1 Example 1 (determination of $Q_0(x)$ when $Q_1(x)$ is known)

In this example, the inverse initial boundary value problem (2)-(5) and (8) requires to determine both the potential $Q_0(x)$ and the displacement $u(x,t)$ (assuming that $Q_1(x)$ is known and taken for simplicity to be zero), from the governing equation

$$u_{tt} = u_{xx} + Q_0(x)u, \quad (x,t) \in (0,1) \times (0,1), \tag{105}$$

with the input data

$$u(x,0) = \varphi(x) = 2 + \cos(\pi x), \quad u_t(x,0) = \psi(x) = 2 + \cos(\pi x), \quad x \in [0,1], \tag{106}$$

$$-\frac{\partial u}{\partial x}(0,t) = q_0(t) = 0, \quad \frac{\partial u}{\partial x}(1,t) = q_L(t) = 0, \quad t \in (0,1], \tag{107}$$

$$u(0,t) = P_0(t) = 3e^t, \quad u(1,t) = P_1(t) = e^t, \quad t \in [0,1]. \tag{108}$$

Remark that the Neumann boundary conditions (107) are homogenous and that the initial data (106) satisfy conditions (10) and (13). Then, Lemma 1 and Theorem 1 are applicable for the direct and inverse problems (105)-(107) and (105)-(108), respectively. In particular, it follows that the inverse problem (105)-(108) is uniquely solvable and, in fact, it can easily be checked that its exact solution is given by

$$u(x,t) = e^t(\cos(\pi x) + 2), \quad (x,t) \in [0,1] \times [0,1]. \tag{109}$$

$$Q_0(x) = \frac{2 + (1+\pi^2)\cos(\pi x)}{2 + \cos(\pi x)}, \quad x \in [0,1]. \tag{110}$$

First, before we attempt the inversion, it is worth to assess the convergence and accuracy of the FDM direct solver described in Section 4. Therefore, solving the direct problem (105)-(107) when Q_0 is assumed known and given by (110) we obtain the numerical results for the

boundary Dirichlet data presented in Figure 1 for various $N = M \in \{5, 10, 20\}$ in comparison with the exact solutions (108). From this figure a rapid monotonically increasing convergence of the numerical solutions to their exact targets (108) and excellent accuracy can be observed (in fact the numerical results obtained with $N = M = 10$ and 20 are undistinguishable).

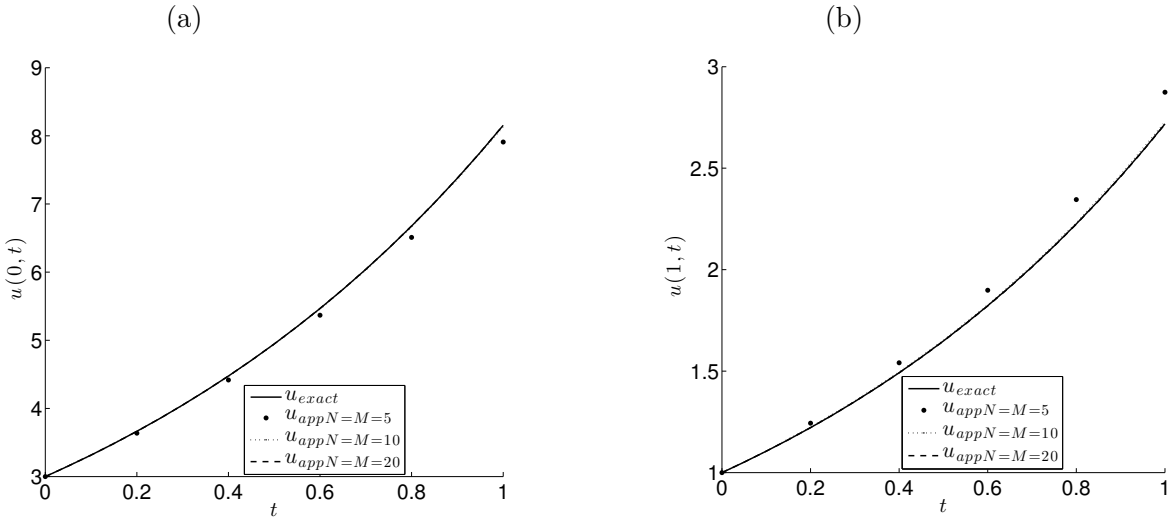

Figure 1: The exact solutions (a) $u(0,t) = 3e^t$, (b) $u(1,t) = e^t$ in comparison with the numerical solutions for various $N = M \in \{5, 10, 20\}$, for the direct problem of Example 1.

Next, we attempt solving numerically the inverse problem (105)-(108) by minimizing the least-squares objective function

$$\mathcal{F}(\underline{Q}_0) := \sum_{j=1}^{N} (u(0, t_j; \underline{Q}_0) - P_0(t_j))^2 + \sum_{j=1}^{N} (u(1, t_j; \underline{Q}_0) - P_1(t_j))^2, \tag{111}$$

using the routine *lsqnonlin* described in Section 5 starting with the initial guess zero. Remark that when both Dirichlet data in (108) are measured this corresponds to the full data measurement (5) and minimizing (111) imposes $2N$ constraints in M unknowns. In this subsection, we also investigate the case when we only measure partially the data in (108) in which case we minimize the partial least-squares objective function

$$\mathcal{F}_{partial}(\underline{Q}_0) := \sum_{j=1}^{N} (u(0, t_j; \underline{Q}_0) - P_0(t_j))^2. \tag{112}$$

In this case, minimizing (112) imposes N constraints in M unknowns.

For exact data (108), the results are depicted in Figure 2. From this figure it can be seen that the numerical solution for $Q_0(x)$ converges to the exact solution (110), as the FDM mesh size decreases, and there is not much difference in the excellently obtained accuracy when using both data in (108) or, when using the partial data in (108) alone. This is true for exact data and confirms the theory of subsection 3.1, but for noisy data which we consider next the accuracy of the solution changes significantly, as described below.

We consider therefore solving the inverse problem with fixed $N = M = 20$ but with noise included in the Dirichlet boundary measured data (108), as described in (104). This

is numerically simulated by

$$P_i^{\epsilon}(t_j) = P_i(t_j) + \epsilon_j^i, \quad j = \overline{1,N}, \quad i = 0,1, \tag{113}$$

where $(\epsilon_j^i)_{j=\overline{1,N}}$ are N random noisy variables generated using the MATLAB command 'normrd' from a Gaussian normal distribution with mean zero and standard deviation $\sigma_i = p \times \max_{t\in[0,T]} |P_i(t)|$ for $i = 0, 1$, where p represents the percentage of noise.

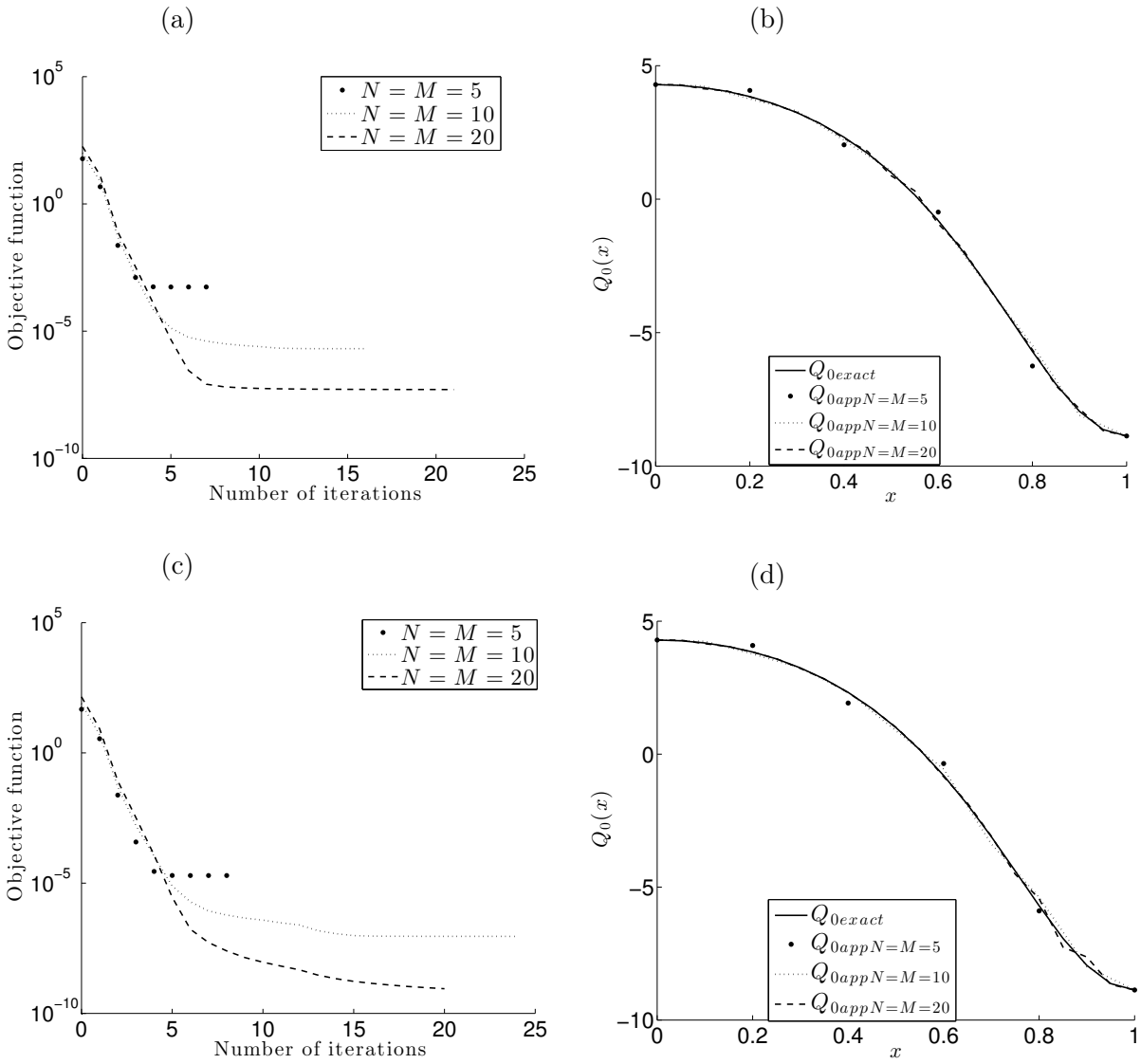

Figure 2: (a) The objective function (111), as a function of the number of iterations, and (b) the exact solution (110) for the coefficient $Q_0(x)$ in comparison with the numerical solutions, for various $N = M \in \{5, 10, 20\}$, no noise for the inverse problem of Example 1. Figures (c) and (d) represent the same quantities as (a) and (b), but obtained by minimizing the partial objective function (112) instead of (111).

In order to investigate the stability of the numerical solution we include $p \in \{1, 3, 5\}\%$ noise into the input data (108), as given in (113). In this case the perturbed noisy data (104) replaces the exact data in (111). The numerical solutions for $Q_0(x)$ obtained by minimizing

(111) or (112) with no regularization are plotted in Figure 3. It can be clearly seen that very high and unbounded oscillations appear. This clearly shows that the ICIP's under investigation are ill-posed. In order to deal with this instability we employ the Tikhonov regularization which minimizes the penalised least-squares functional

$$\mathcal{F}_\lambda(\underline{Q}_0) := \mathcal{F}(\underline{Q}_0) + \lambda \sum_{i=1}^{M} Q_{0i}^2, \tag{114}$$

or, its partial version

$$\mathcal{F}_{partial,\lambda}(\underline{Q}_0) := \mathcal{F}_{partial}(\underline{Q}_0) + \lambda \sum_{i=1}^{M} Q_{0i}^2, \tag{115}$$

where $\lambda > 0$ is a regularization parameter to be prescribed. Including regularization we obtain the numerical solutions presented in Figure 5, whose accuracy errors

$$E_0 := \sqrt{\frac{1}{M} \sum_{i=1}^{M} (Q_{0exact}(x_i) - Q_{0app}(x_i))^2}, \tag{116}$$

as functions of λ, are plotted in Figure 4. From Figure 4 it can be seen that the minimum of the error occurs around $\lambda = 0.05$ for $p = 1\%$ and $\lambda = 0.1$ for $p \in \{3, 5\}\%$. Other than that, the regularization parameter can also be chosen by trial and error. By plotting the numerical solution for various values of λ we can infer when the instability starts to kick off.

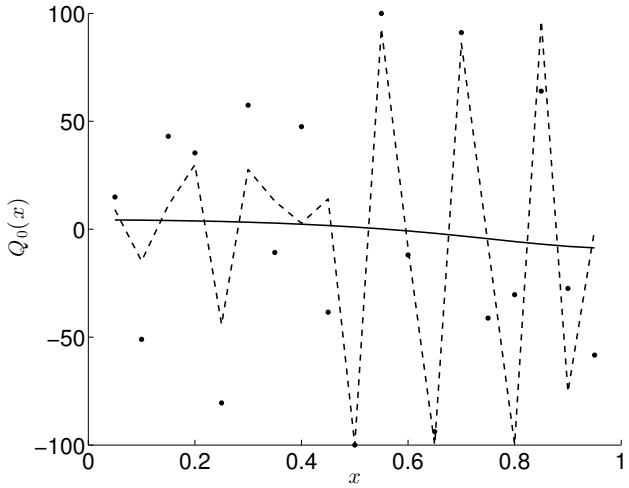

Figure 3: The exact solution (110) (—) for the coefficient $Q_0(x)$ in comparison with the numerical solutions obtained by minimizing (111) (- - -) or (112) (•••), with no regularization, for $p = 1\%$ noisy data for the inverse problem of Example 1.

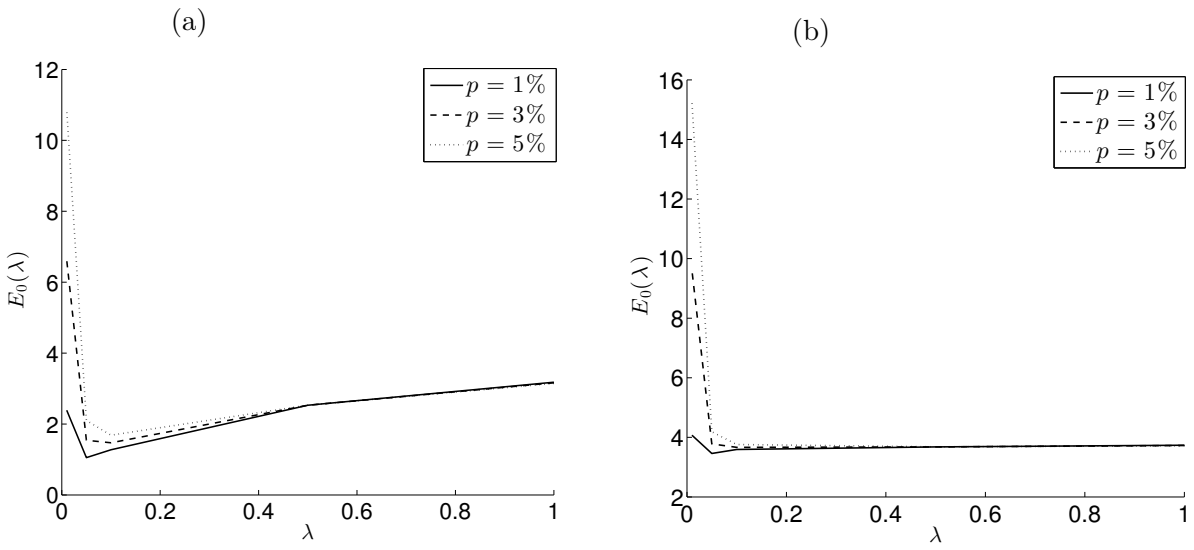

Figure 4: The accuracy error E_0, as a function of λ, for $p \in \{1, 3, 5\}\%$ noise, for the inverse problem of Example 1, obtained by minimizing: (a) the functional (114) and (b) the partial functional (115).

Figure 5 shows the regularized numerical solution for $Q_0(x)$ obtained for $p \in \{1, 3, 5\}\%$ noisy data. From Figures 5(a) and 5(c) it looks like it may be possible to stop after just 2 or 3 iterations because the objective function is no longer significantly decreasing. We note however that because we are already including a positive regularization parameter $\lambda > 0$ in the minimization of (114) or (115), there is no need to stop the iterations at an appropriate threshold, as usually happens with semi-convergent iterative regularization methods, see Hao *et al.* (2012). From Figure 5(b) it can be seen that the numerical results are stable and they become more accurate as the amount of noise p decreases. Also, by comparing Figures 5(b) and 5(d) it can be clearly seen that adding more information to the inverse problem, i.e. using the Dirichlet data (108) at both endpoints $x \in \{0, 1\}$ instead of only at $x = 0$, improves significantly the accuracy of the reconstruction.

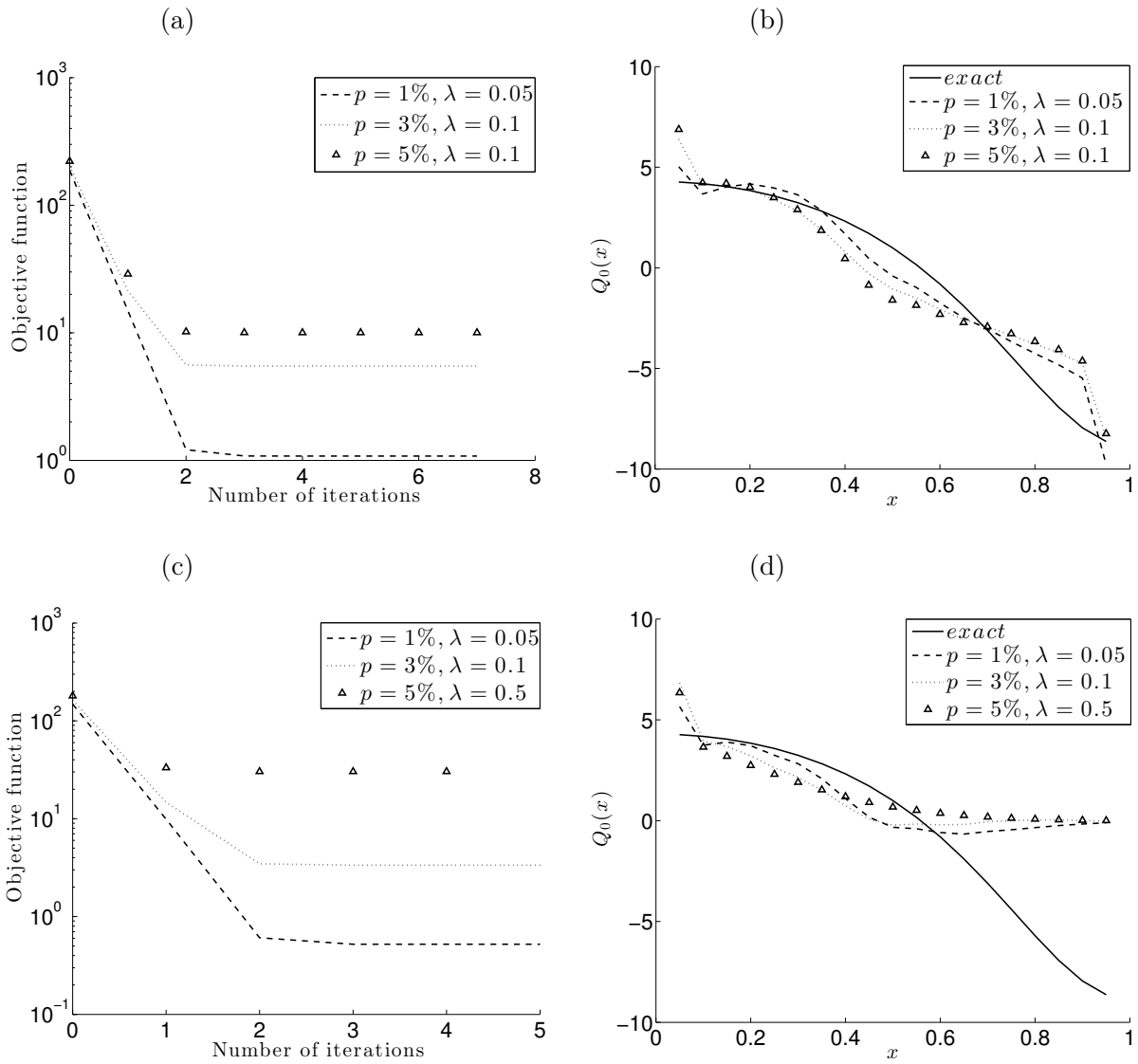

Figure 5: (a) The regularized objective function (114), as a function of the number of iterations, and (b) the exact solution (110) for the coefficient $Q_0(x)$ in comparison with the numerical solutions, for $p \in \{1, 3, 5\}\%$ noise, for the inverse problem of Example 1. Figures (c) and (d) represent the same quantities as (a) and (b), but obtained by minimizing the partial regularized objective function (115) instead of (114).

In the remaining of this section we will only consider, for brevity, the global Cauchy data prescription given by the Dirichlet and Neumann data (4) and (5) (when $\Gamma_0 = \partial\Omega$ in (31)).

6.2 Example 2 (determination of $Q_1(x)$ when $Q_0(x)$ is known)

In this example, the inverse initial boundary value problem (2)-(5) and (37) requires to determine both the damping term $Q_1(x)$ and the displacement $u(x,t)$ (assuming that $Q_0(x)$ is known and taken for simplicity to be zero), from the governing equation

$$u_{tt} = u_{xx} + Q_1(x)u_t, \quad (x,t) \in (0,1) \times (0,1), \tag{117}$$

with the same input data (106)-(108). One can observe that the conditions of Theorem 3 are satisfied hence the solution of the inverse problem (106)-(108) and (117) is unique. Moreover, one can easily check that the solution $(u(x,t), Q_1(x))$ is given by equation (109) for $u(x,t)$, whilst for $Q_1(x)$ has the same expression as that of equation (110), namely,

$$Q_1(x) = \frac{2 + (1+\pi^2)\cos(\pi x)}{2 + \cos(\pi x)}, \quad x \in [0,1]. \tag{118}$$

We attempt solving numerically the inverse problem (106)-(108) and (117) by minimizing the least-squares objective function

$$\mathcal{F}(\underline{Q}_1) := \sum_{j=1}^{N} (u(0,t_j;\underline{Q}_1) - P_0(t_j))^2 + \sum_{j=1}^{N} (u(1,t_j;\underline{Q}_1) - P_1(t_j))^2, \tag{119}$$

using the routine *lsqnonlin* described in Section 5 starting with the initial guess zero.

For exact data (108), the results are depicted in Figure 6 and similar convergent results as those obtained in Figure 2 for Example 1 can be observed.

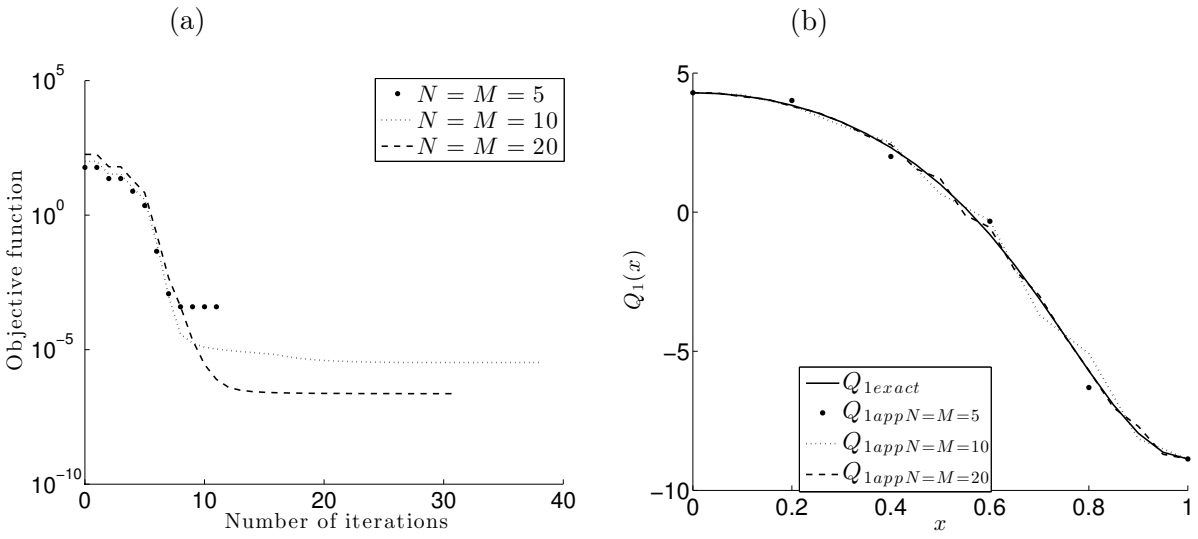

Figure 6: (a) The objective function (119), as a function of the number of iterations, and (b) the exact solution (118) for the coefficient $Q_1(x)$ in comparison with the numerical solutions, for various $N = M \in \{5, 10, 20\}$, no noise for the inverse problem of Example 2.

Next, we fix $M = N = 20$ and add $p = 1\%$ noise in the Dirichlet boundary data (108), as given in (113). As shown in Figure 7, the unregularized numerical solution obtained by minimizing (119) is seen to be highly unstable. This is similar to the unstable behaviour of the numerical results shown with dashed line (- - -) in Figure 3 for Example 1, though the amplitude of the oscillations in Figure 7 for Example 2 is about 3 times lower than that for Example 1.

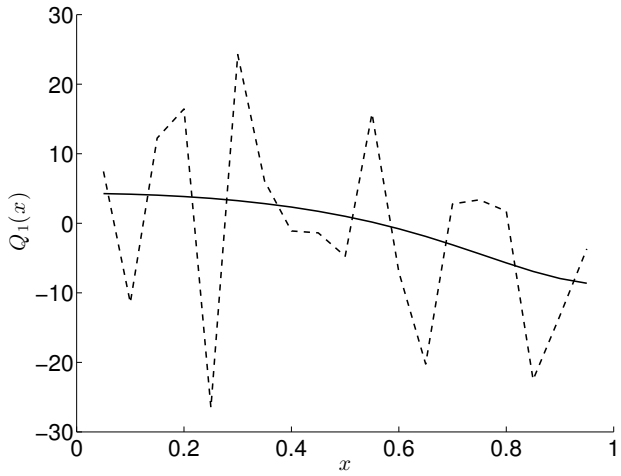

Figure 7: The exact solution (118) (—) for the coefficient $Q_1(x)$ in comparison with the numerical solution (- - -), with no regularization, for $p = 1\%$ noisy data for the inverse problem of Example 2.

As for Example 1, in order to stabilise the solution the functional (119) is regularized and this recasts into minimizing the penalised least-squares functional

$$\mathcal{F}_\lambda(\underline{Q}_1) := \mathcal{F}(\underline{Q}_1) + \lambda \sum_{i=1}^{M} Q_{1i}^2. \tag{120}$$

The accuracy error defined as

$$E_1 := \sqrt{\frac{1}{M} \sum_{i=1}^{M} (Q_{1exact}(x_i) - Q_{1app}(x_i))^2}, \tag{121}$$

as a function of λ, is plotted in Figure 8 for $p \in \{1, 3, 5\}\%$ noise and similar behaviour to that illustrated in Figure 4 for Example 1 can be observed. Based on Figure 8 or on trial and error, with a suitable choice of the regularization parameter λ depending on the amount of noise p, stable numerical results are obtained, as illustrated in Figure 9. Nevertheless, criteria such as the L-curve method, see Hansen (2001), which plots the residual $\sqrt{\mathcal{F}(\underline{Q}_1)}$ versus the solution norm $\|\underline{Q}_1\|$ for various values of $\lambda > 0$, could also be employed to select an appropriate value of the regularization parameter at the corner of the L-curve (if obtained), as described elsewhere, see e.g. Huntul *et al.* (2017).

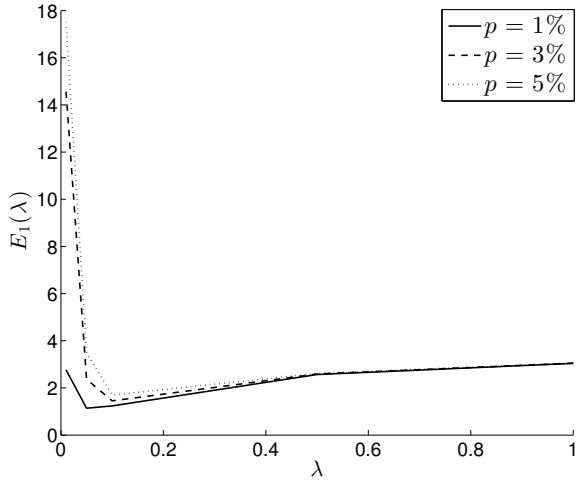

Figure 8: The accuracy error E_1, as a function of λ, for $p \in \{1, 3, 5\}\%$ noise, for the inverse problem of Example 2.

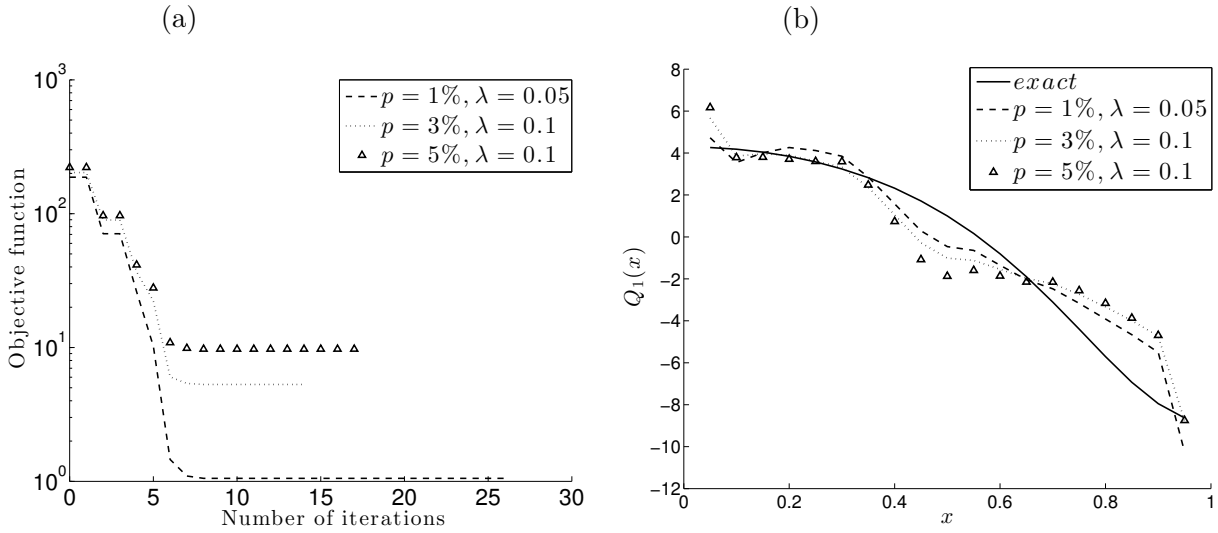

Figure 9: (a) The regularized objective function (120), as a function of the number of iterations, and (b) the exact solution (118) for the coefficient $Q_1(x)$ in comparison with the numerical solutions, for $p \in \{1, 3, 5\}\%$ noise and regularization parameters $\lambda \in \{0.05, 0.1\}$, for the inverse problem of Example 2.

6.3 Example 3 (determination of $Q_0(x)$ and $Q_1(x)$)

In this example, the inverse initial boundary value problem (1)-(5) requires to determine the potential $Q_0(x)$, the damping term $Q_1(x)$ and the displacement $u(x,t)$ from the governing equation

$$u_{tt} = u_{xx} + +Q_0(x)u + Q_1(x)u_t, \quad (x,t) \in (0,1) \times (0,1), \tag{122}$$

with the homogeneous flux data (107) and

$$u(x,0) = \varphi(x) = 0, \quad u_t(x,0) = \psi(x) = 2 + \cos(\pi x), \quad x \in [0,1], \tag{123}$$

$$u(0,t) = P_0(t) = 3(e^t - 1), \quad u(1,t) = P_1(t) = e^t - 1, \quad t \in [0,1]. \tag{124}$$

One can easily check that the triplet solution $(u(x,t), Q_0(x), Q_1(x))$ of the inverse problem (107), (122)-(124) is given by

$$u(x,t) = (e^t - 1)(\cos(\pi x) + 2), \quad (x,t) \in [0,1] \times [0,1]. \tag{125}$$

$$Q_0(x) = \frac{\pi^2 \cos(\pi x)}{2 + \cos(\pi x)}, \quad x \in [0,1]. \tag{126}$$

$$Q_1(x) = 1, \quad x \in [0,1]. \tag{127}$$

We attempt solving numerically the inverse problem (107), (122)-(124), by minimizing the least-squares objective function

$$\mathcal{F}(\underline{Q}_0; \underline{Q}_1) := \sum_{j=1}^{N} (u(0,t_j; \underline{Q}_0; \underline{Q}_1) - P_0(t_j))^2 + \sum_{j=1}^{N} (u(1,t_j; \underline{Q}_1; \underline{Q}_1) - P_1(t_j))^2, \tag{128}$$

using the routine *lsqnonlin* described in Section 5 starting with the initial guess zero.

For exact data (124), the results are depicted in Figure 10. From this figure it can be seen that the numerical solution for $Q_0(x)$ and $Q_1(x)$ converges to the exact solution (126) and (127), respectively, as the FDM mesh size decreases.

Next we consider solving the inverse problem with fixed $N = M = 40$ but with $p = 1\%$ noise included in the Dirichlet boundary data (124), as given in (113). As shown in Figure 11, the unregularized numerical solutions for both $Q_0(x)$ and $Q_1(x)$ obtained by minimizing (128) is seen to be highly unstable.

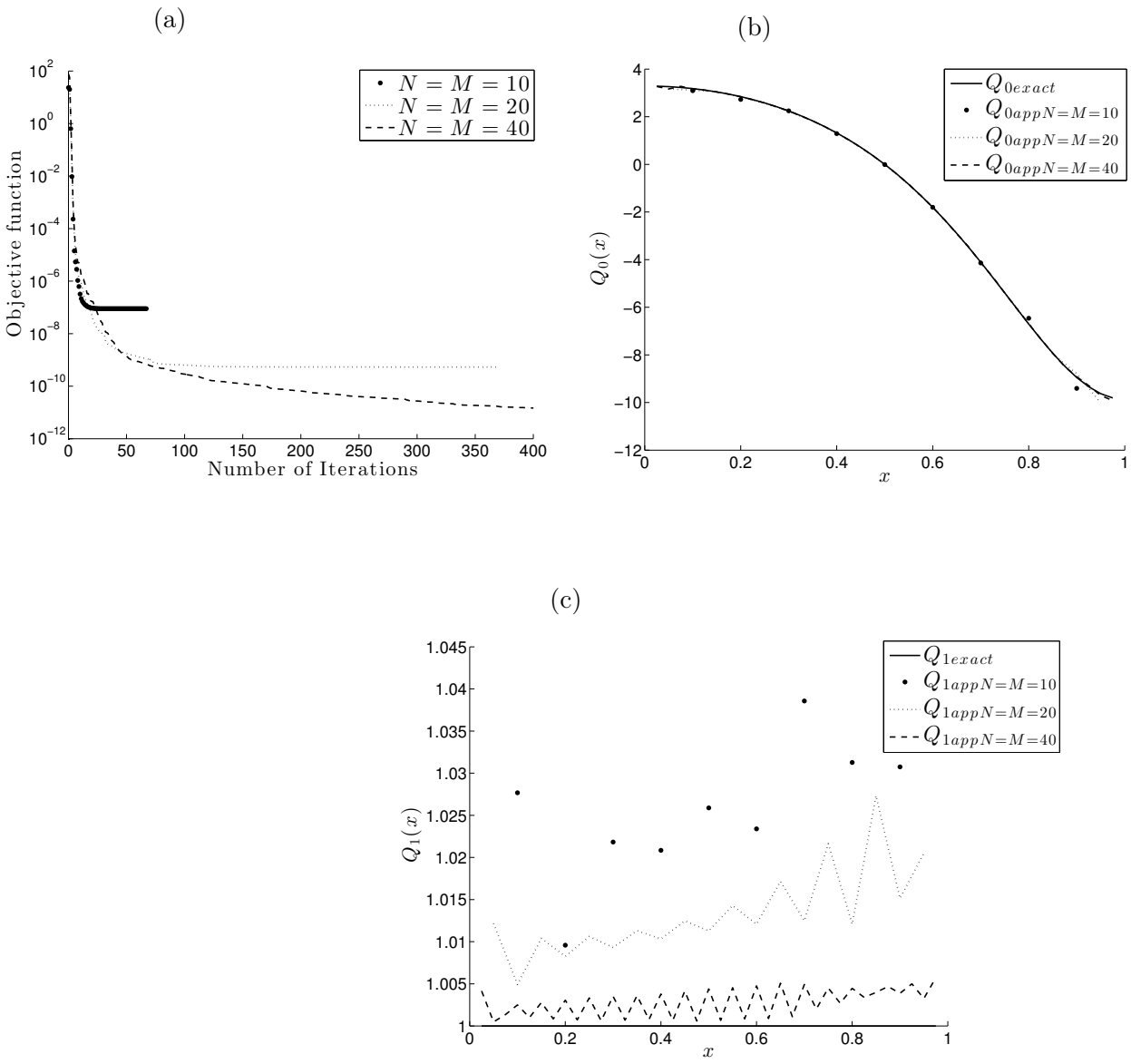

Figure 10: (a) The objective function (128), as a function of the number of iterations, (b) the exact solution (126) for $Q_0(x)$ and (c) the exact solution (127) for $Q_1(x)$ in comparison with the numerical solutions, for various $N = M \in \{10, 20, 40\}$, no noise for the inverse problem of Example 3.

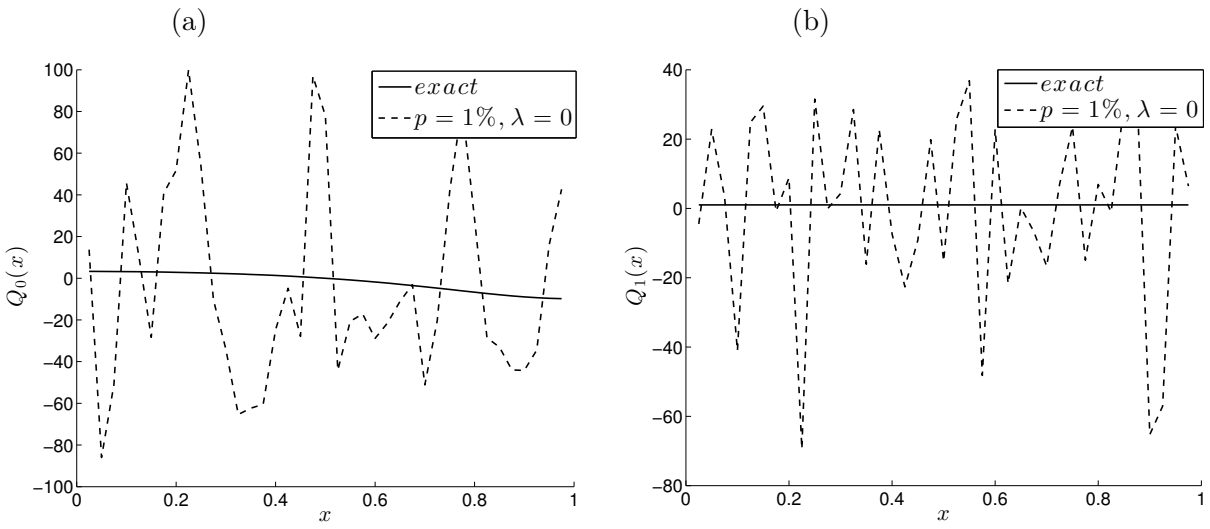

Figure 11: The exact solutions given by (a) equation (126) and (b) equation (127) for the coefficients $Q_0(x)$ and $Q_1(x)$, respectively, in comparison with the numerical solutions, with no regularization, for $p = 1\%$ noisy data for the inverse problem of Example 3.

In order to stabilise the solution, the functional (128) is regularized and this recasts into minimizing the penalised least-squares functional

$$\mathcal{F}_\lambda(\underline{Q}_0; \underline{Q}_1) := \mathcal{F}(\underline{Q}_0; \underline{Q}_1) + \lambda \sum_{i=1}^{M} Q_{0i}^2 + \lambda \sum_{i=1}^{M} Q_{1i}^2. \tag{129}$$

The numerically obtained results for $p = 1\%$ noise and $\lambda = 0.01$ are illustrated in Figure 12. By comparing the ordinate (y-axis) scale in Figures 11 and 12 the benefit of regularization can be clearly observed. Of course, more rigorous choices of the regularization parameter remain an open issue, and, as preliminary studies, e.g. Huntul *et al.* (2017), indicate it may be well that the objective functional (129) has to be generalised to include two different regularization parameters λ_1 and λ_2 penalising the last two terms in it. However, in this case the simultaneous choice of multiple regularization parameters, see Belge *et al.* (2002) and Fornasier *et al.* (2014), becomes an even harder problem than the previous single parameter case, and therefore is deferred to a future work.

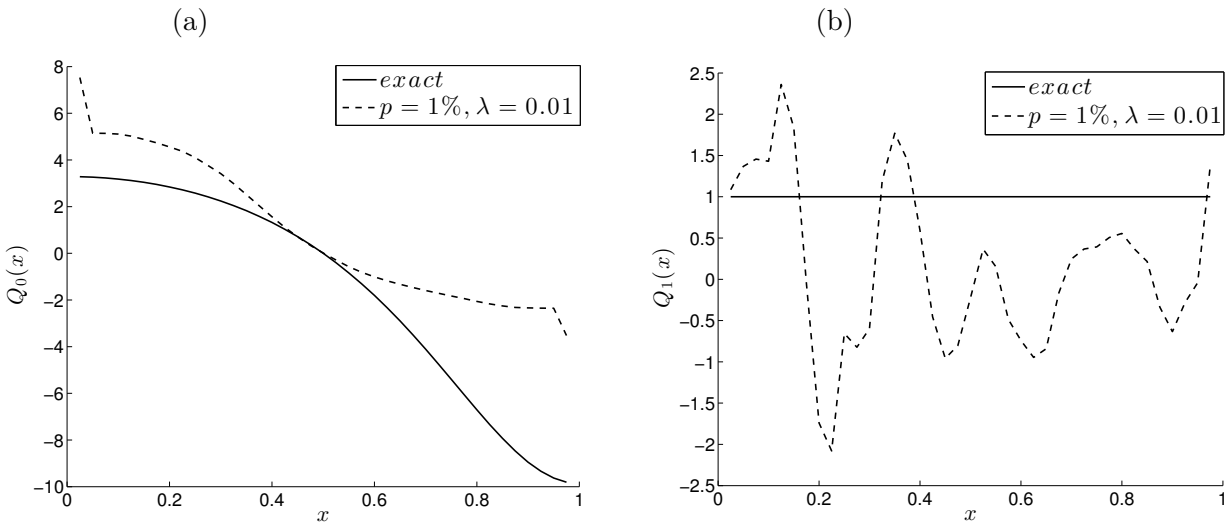

Figure 12: The exact solutions given by (a) equation (126) and (b) equation (127) for the coefficients $Q_0(x)$ and $Q_1(x)$, respectively, in comparison with the numerical solutions, with regularization, for $p = 1\%$ noisy data for the inverse problem of Example 3.

7 Conclusions

In this paper, nonlinear identifications of the space-dependent potential and/or damping coefficients in the wave equation have been investigated. As illustrated in Figures 3, 7 and 11, these inverse coefficient identification problems are ill-posed since small random errors in the input data cause large errors in the output solution. In order to stabilise the solution, the nonlinear Tikhonov regularization method has been employed. The minimization has been performed numerically using the MATLAB toolbox optimization routine *lsqnonlin*. Numerical results presented and discussed for various examples have been concerned with the inverse reconstruction of the coefficient $Q_0(x)$, or $Q_1(x)$, or both $Q_0(x)$ and $Q_1(x)$.

We mention that the numerical techniques of this paper (FDM plus *lsqnonlin* minimization of the Tikhonov functional) have recently been applied successfully in Hussein *et al.* (2014) and Hussein and Lesnic (2016), for solving a similar coefficient identification problem for the heat equation. Therein, many more examples have been tested including successful recoveries of non-smooth coefficients.

In the case of exact data, the numerical results presented in Figures 2(b), 2(d), 6(b) and 10(b), 10(c) show that for all Examples 1-3 the numerical solutions are convergent to their corresponding analytical solutions, as the FDM mesh size decreases, and no regularization is needed.

The case of partial Cauchy data has also been considered in subsection 6.1 for the inverse problem of retrieving the potential $Q_0(x)$. By comparing Figures 2(b) and 2(d) one has observed that in the case of exact data accurate numerical solutions have been obtained in both cases of full or partial Cauchy data being considered. However, for noisy data by comparing Figures 5(b) and 5(d) one has observed that, as expected, the full Cauchy data provide more (significant) information than the partial Cauchy data.

Another comparison was made by observing Figures 5(b) and 9(b) corresponding to the identification of the potential $Q_0(x)$ and the damping coefficient $Q_1(x)$, respectively. From

these figures it has been seen that there was no major difference between the two regularized solutions in terms of stability and accuracy.

A final inverse problem consisted in simultaneously identifying both $Q_0(x)$ and $Q_1(x)$, as performed in subsection 6.3. As expected, this is a more difficult problem than the separate single identification of the coefficient $Q_0(x)$ or $Q_1(x)$, as performed in subsections 6.1 and 6.2, respectively. A complete uniqueness theorem for this problem given by (1)-(5) with a single choice of initial data (2) and (3) which must also satisfy non-zero conditions for the technique of Carleman estimates to be applicable is still missing, but it is hoped that this would be possible to formulate and prove in an immediate future work. At this stage, at least numerically, for exact data, Figures 10(b) and 10(c) have shown that both coefficients can be retrieved accurately, but for noisy data, Figures 12(a) and 12(b) have showed that the accuracy and stability deteriorate. On the other hand, comparison of Figures 11 and 12 has showed that the use of regularization significantly alleviates the highly unbounded and oscillatory numerical reconstructions obtained when no regularization was employed.

Future work will be concerned with the reconstruction of the vectorial function $Q_2(x)$ in the wave equation $u_{tt} = \nabla^2 u + Q_0(x)u + Q_1(x)u_t + Q_2(x) \cdot \nabla u$.

Acknowledgments

S.O. Hussein would like to thank the financial support received from the Human Capacity Development Programme (HCDP) in Kurdistan for performing her PhD at the University of Leeds. M. Yamamoto is partly supported by a Grant-in-Aid for Scientific Research (S) No. 15H05740 and A3 Foresight Program "Modeling and Computation of Applied Inverse Problems" by the Japan Society for the Promotion of Science (JSPS). The authors would like to thank the referees for their useful comments.

References

[1] Adams, R.A. *Sobolev Spaces*, Academic Press, New York, 1978.

[2] Baudouin, L. *Lipschitz stability in an inverse problem for the wave equation*, https://hal.archives-ouvertes.fr/hal-00598876/fr/, 2011.

[3] Baudouin, M., de Buhan, M. and Ervedoza, S. *Global Carleman estimates for waves and applications*, Communications in Partial Differential Equations, **38**, 823-859, 2013.

[4] Beilina, L. and Klibanov, M.V. *Approximate Global Convergence and Adaptivity for Coefficient Inverse Problems*, Springer, New York, 2012.

[5] Belge, M., Kilmer, M. and Miller, E. *Efficient determination of multiple regularization parameters in a generalized L-curve framework*, Inverse Problems, **18**, 1161-1183, 2002.

[6] Bellassoued, M. and Yamamoto, M. *Carleman Estimates and Applications to Inverse Problems for Hyperbolic Systems*, Springer Monographs in Mathematics, Springer-Verlag, Berlin, 2017, to appear.

[7] Bukhgeim, A. L. and Klibanov, M. V. *Global uniqueness of a class of multidimensional inverse problems*, Soviet Mathematics Doklady, **24**, 244-247, 1981.

[8] Bukhgeim, A.L., Cheng, J., Isakov, V. and Yamamoto, M. *Uniqueness in determining damping coefficients in hyperbolic equations*, In: Analytic Extension Formulas and Their Applications, (eds. S. Saitoh, N. Hayashi and M. Yamamoto), Kluwer Academic Publishers, Dordrecht, 27-46, 2001.

[9] Cannon, J.R. and Dunninger, D.R. *Determination of an unknown forcing function in a hyperbolic equation from overspecified data*, Annali di Matematical Pura ed Applicata, **1**, 49-62, 1970.

[10] Cannon, J.R. and DuChateau, P. *An inverse problem for an unknown source term in a wave equation*, SIAM Journal on Applied Mathematics, **43**, 553-564, 1983.

[11] Chow, Y.T. and Zou, J. *A numerical method for reconstructing the coefficient in a wave equation*, Numerical Methods for Partial Differential Equations, **31**, 289-307, 2014.

[12] Coleman, T.F. and Li, Y. *On the convergence of interior-reflective Newton methods for nonlinear minimization subject to bounds*, Mathematical Programming, **67**, 189-224, 1994.

[13] Collins, M.D. and Kuperman, W.A. *Inverse problems in ocean acoustics*, Inverse Problems, **10**, 1023-1040, 1994.

[14] Engl, H.W., Scherzer, O. and Yamamoto, M. *Uniqueness and stable determination of forcing terms in linear partial differential equations with overspecified boundary data*, Inverse Problems, **10**, 1053-1076, 1994.

[15] Fornasier, M., Naumova, V. and Pereverzyev, S.V. *Parameter choice strategies for multipenalty regularization*, SIAM Journal on Numerical Analysis, **52**, 1770-1794, 2014.

[16] Hansen, P.C. *The L-curve and its use in the numerical treatment of inverse problems*, in Computational Inverse Problems in Electrocardiology, (ed. P. Johnston), WIT Press, Southampton, 119-142, 2001.

[17] Hao, D.N., Thanh, P.X., Lesnic, D. and Johansson, B.T. *A boundary element method for a multi-dimensional inverse heat conduction problem*, International Journal of Computer Mathematics, **89**, 1540-1554, 2012.

[18] Huang, C.H. *An inverse non-linear force vibration problem of estimating the external forces in a damped system with time-dependent system parameters*, Journal of Sound and Vibration, **242**, 749-765, 2001.

[19] Huntul, M.J., Lesnic, D. and Hussein, M.S. *Reconstruction of time-dependent coefficients from heat moments*, Applied Mathematics and Computation, **301**, 233-253, 2017.

[20] Hussein, M.S., Lesnic, D. and Ivanchov, M.I. *Simultaneous determination of time-dependent coefficients in the heat equation*, Computers and Mathematics with Applications, **67**, 1065-1091, 2014.

[21] Hussein, M.S. and Lesnic, D. *Simultaneous determination of time and space-dependent coefficients in a parabolic equation*, Communications in Nonlinear Science and Numerical Simulation, **33**, 194-217, 2016.

[22] Hussein, S.O. and Lesnic, D. *Determination of a space-dependent source function in the one-dimensional wave equation*, Electronic Journal of Boundary Elements, **12**, 1-26, 2014.

[23] Hussein, S.O. and Lesnic, D. *Determination of forcing functions in the wave equation. Part I: the space-dependent case*, Journal of Engineering Mathematics, **96**, 115-133, 2016.

[24] Imanuvilov, O.Yu. and Yamamoto, M. *Global uniqueness and stability in determining coefficients of wave equations*, Communications in Partial Differential Equations, **26**, 1409-1425, 2001a.

[25] Imanuvilov, O.Yu. and Yamamoto, M. *Global Lipschitz stability in an inverse hyperbolic problem by interior observations*, Inverse Problems, **17**, 717-728, 2001b.

[26] Ito, K. and Liu, J.-C. *Recovery of inclusions in 2D and 3D domains for poisson's equation*, Inverse Problems, **29**, 075005 (20 pages), 2013.

[27] Klibanov, M.V. *Inverse problems and Carleman estimates*, Inverse Problems, **8**, 575-596, 1992.

[28] Klibanov, M.V. *Carleman estimates for global uniqueness, stability and numerical methods for coefficient inverse problems*, Journal of Inverse and Ill-Posed Problems, **21**, 477-560, 2013.

[29] Lions, J.L. and Magenes, E. *Non-homogenous Boundary Value Problems and Applications*, Vol. I, Springer-Verlag, Berlin, 1972.

[30] Lions, J.-L. *Contrôlabilité Exacte Perturbations et Stabilisation de Systèmes Distribués*, Vol. I, Masson, Paris, 1988.

[31] Liu, S. and Triggiani, R. *Global uniqueness and stability in determining the damping and potential coefficients of an inverse hyperbolic problem*, Nonlinear Analysis: Real World Applications, **12**, 1562-1590, 2011.

[32] Liu, S. and Triggiani, R. *Recovering damping and potential coefficients for an inverse non-homogeneous second-order hyperbolic problem via a localized Neumann boundary trace*, Discrete and Continuous Dynamical Systems, **33**, 5217- 5252, 2013.

[33] Puel, J.-P. and Yamamoto, M. *On a global estimate in a linear hyperbolic problem*, Inverse Problems, **12**, 995-1002, 1996.

[34] Sjogreen, B. and Petersson, N.A. *Source estimation by full wave form inversion*, Journal of Scientific Computing, **59**, 247-276, 2014.

[35] Smith, G.D. *Numerical Solution of Partial Differential Equations: Finite Difference Methods*, Clarendon Press, Oxford, 3rd edn., 1985.

[36] Sun, Z. *On continuous dependence for an inverse initial boundary value problem for the wave equation*, Journal of Mathematical Analysis and Applications, **150**, 188-204, 1990.

[37] Yamamoto, M. *Stability, reconstruction formula and regularization for an inverse source hyperbolic problem by a control method*, Inverse Problems, **11**, 481-496, 1995.

[38] Yamamoto, M. *Uniqueness and stability in multidimensional hyperbolic inverse problems*, Journal de Mathématiques Pures et Appliquées, **78**, 65-98, 1999.